



universität
wien

MASTERARBEIT

Titel der Masterarbeit

„Identification of histones as phospho-tyrosine targets of the
ALK kinase in anaplastic large cell lymphoma (ALCL)“

Verfasserin

Julia Hacker, BSc

angestrebter akademischer Grad

Master of Science (MSc)

Wien, 2013

Studienkennzahl lt.
Studienblatt:

A 066 877

Studienrichtung lt.
Studienblatt:

Masterstudium Genetik und Entwicklungsbiologie

Betreuerin:

Ass. Prof. Dr. Gerda Egger

Table of contents

1	ABSTRACT	9
2	ZUSAMMENFASSUNG	11
3	INTRODUCTION	13
3.1	Anaplastic large cell lymphoma	13
3.2	The role of NPM-ALK in ALK+ ALCL	13
3.2.1	Anaplastic lymphoma kinase (ALK).....	14
3.2.2	Nucleophosmin (NPM).....	14
3.2.3	ALK signaling.....	15
3.3	General role of ALK in cancer	16
3.4	Therapeutic approaches	17
3.5	Histone modifications	18
3.6	Histone tyrosine phosphorylation	18
3.6.1	Tyrosine residues in core histones.....	20
3.6.2	Phosphorylation on H2A.X Y142 regulates DNA repair and apoptosis.....	20
3.6.3	Tyrosine 41 on H3 is phosphorylated by JAK2 in hematopoietic cells.....	21
3.6.4	Histone H3 Y99 phosphorylation regulates histone proteolysis in yeast.....	22
3.6.5	H2B Y37 phosphorylation suppresses expression of histone genes.....	22
3.6.6	Future perspectives.....	23
3.7	Project description and hypothesis	24
4	MATERIALS AND METHODS	26
4.1	Cell culture	26
4.2	Inhibitor treatments	26
4.3	Whole cell protein extraction	26
4.3.1	Buffers.....	26
4.3.2	Protocol.....	27
4.4	Histone isolation	27
4.4.1	Buffers.....	27
4.4.2	Protocol.....	28
4.5	Preparation of nuclear and cytoplasmic protein extracts	28
4.5.1	Buffers.....	28
4.5.2	Protocol.....	29
4.6	Isolation of peripheral blood mononuclear cells (PBMCs)	30
4.7	Western Blotting	30

4.7.1	Buffers	30
4.7.2	Protocol	31
4.7.3	SDS-polyacrylamide gels	32
4.8	Immunofluorescence staining	32
4.9	Immunoprecipitation	33
4.9.1	Buffers	33
4.9.2	Protocol	34
4.10	Cell synchronization by double thymidine block	34
4.11	PI staining and flow cytometry	35
4.12	Kinase assays	35
4.12.1	Buffers	35
4.12.2	Protocol	36
4.13	Antibodies	36
4.13.1	Primary Antibodies	36
4.13.2	Secondary Antibodies	37
4.14	Bioinformatic analysis	37
5	RESULTS	38
5.1	Identification of ALK in the nucleus	38
5.2	Characterization of histone tyrosine phosphorylation in ALK+ ALCL cells	41
5.3	<i>In vitro</i> kinase assays	44
5.4	<i>In silico</i> analysis of histone tyrosine phosphorylation	46
6	DISCUSSION	48
6.1	Identification of ALK in the nucleus	48
6.2	Characterization of histone tyrosine phosphorylation in ALK+ ALCL cells	49
6.3	<i>In vitro</i> kinase assays	50
6.4	<i>In silico</i> analysis of histone tyrosine phosphorylation	51
6.5	Conclusion	52
6.6	Outlook	53
7	REFERENCES	54
8	APPENDIX	61
8.1	Acknowledgements	61
8.2	Curriculum Vitae	63

Table of figures

Figure 1: Schematic view of full-length ALK and NPM and the NPM-ALK fusion protein. In NPM-ALK, the extracellular region of ALK is lost and replaced by the N-terminal region of NPM containing the oligomerization domain, which enables the formation of heterodimers and activation of downstream signaling pathways. 14

Figure 2: Molecular network interacting with NPM-ALK in ALK+ ALCL involving signaling pathways like JAK-STAT, PLC- γ , mTOR or Pi3K-AKT [2]. 15

Figure 3: Overview of ALK in cancer. ALK fusion proteins (in beige) have been described in anaplastic large cell lymphoma (ALCL), inflammatory myofibroblastic tumor (IMT), non-small-cell lung cancer (NSCLC), diffuse large B cell lymphoma (DLBCL), oesophageal squamous cell carcinoma (ESCC), renal medulla carcinoma (RMC), renal cell carcinoma (RCC), breast cancer, colon carcinoma and serous ovarian carcinoma (SOC). ALK overexpression (pink) is yet not fully understood but has been reported in various cancer types. The third category are ALK point mutations (blue), which comprise both primary tumour-associated mutations and secondary mutations in Crizotinib-resistant patients. Secondary mutations have been described in NSCLC, IMT and anaplastic thyroid cancer (ATC). Primary point mutations are mainly found in neuroblastoma [40]. 16

Figure 4: Overview of tyrosine residues in histones from budding yeast and mammals. The four yeast core histones are marked by the prefix “Sc” and denoted in blue. Mammalian histones are shown in black. The number of amino acid residues (aa) in each histone are noted on the right. The cylinders mark the location of α -helices. Tyrosine residues are shown as balloons. Red balloons mark the tyrosine residues essential for viability in budding yeast. Yellow explosion signs and a “P” mark tyrosine residues that have been shown to be phosphorylated in vivo. Tyrosines that are predicted to be accessible in the nucleosome and can therefore be potentially phosphorylated are indicated by a yellow circle. Solid lines indicate higher probability of phosphorylation, while dashed lines indicate lower probability. Modified after [67]. 19

Figure 5: Model of JAK2 dependent phosphorylation of H3 Y41. In healthy cells JAK2 levels are tightly regulated, leading to regulated displacement of HP1 α from chromatin when H3 Y41 is phosphorylated and to heterochromatic repression, suppression of mitotic recombination and sister chromatid cohesion when H3 Y41 is not phosphorylated and HP1 α is bound to chromatin. Dysregulated JAK2 expression leads to sustained displacement of HP1 α from chromatin, which increases the expression of oncogenes like *LMO2* and probably also promotes mitotic recombination and chromosomal dysjunctions and aneuploidy, thereby driving the cell into oncogenesis [65]. 21

Figure 6: Model of H2B Y37 phosphorylation upstream of the histone gene cluster *Hist1*. WEE1 phosphorylates H2B at Y37 upstream of *Hist1*. NPAT is unable to recognize Y37-phosphorylated H2B and thus dissociates from chromatin. This in turn inhibits RNA polymerase II (Pol II) recruitment. Subsequently, HIRA is recruited to phosphorylated H2B Y37, preventing rebinding of NPAT and effectively suppressing histone mRNA synthesis [66]. 23

Figure 7: ALK is present in the nucleus of ALK+ ALCL cells. a) Confocal immunofluorescent images show nuclear ALK in Karpas299 and SU-DHL-1 cells. ALK- Mac2a cells do not show any ALK staining. b) Western blotting of

cytoplasmic (C) and nuclear (N) extracts from Karpas299 and SU-DHL-1 cell lines identifies ALK in both cellular fractions, whereas Hdac2 is restricted to the nuclear compartment and GAPDH is enriched in the cytoplasmic fraction. 38

Figure 8: ALK is active in the nucleus of ALK+ ALCL cells. Immunofluorescence staining with an antibody against the active, phosphorylated form of ALK (P-ALK) detects P-ALK in the nuclei of both Karpas299 and SU-DHL-1 cells, but not in ALK- Mac2a cells. 39

Figure 9: ALK is enriched in the nucleoli of ALK+ ALCL cells. Co-Immunofluorescence staining of ALK and the nucleolar protein nucleophosmin (NPM) reveals nucleolar localization of ALK in both Karpas299 and SU-DHL-1 cell lines indicated by overlapping staining patterns. 40

Figure 10: NPM marks nucleoli also in NPM- cells. NPM is a valid nucleolar marker, since it also detects NPM in the ALK- cell line Mac2a, where it shows a similar staining pattern as in ALK+ cells. 40

Figure 11: ALK+ ALCL cells show tyrosine phosphorylation on all core histones. Western blot of acid extracted histones from Karpas299 cells with antibody against P-Tyr shows tyrosine phosphorylation of all core histones. Tyrosine phosphorylation levels were increased by serum stimulation with 20% FCS (fetal calf serum). 41

Figure 12: ALK inhibition reduces levels of histone tyrosine phosphorylation. a) Western blotting of whole cell protein extracts reveals that treatment of Karpas299 cells with Crizotinib inhibits phosphorylation of ALK and STAT3. b) Histone tyrosine phosphorylation is significantly reduced after Crizotinib treatment compared to the DMSO control. 42

Figure 13: PBMCs from healthy controls show lower histone tyrosine phosphorylation levels than ALK+ ALCL cells. Histones were isolated from PBMCs of a healthy control and Karpas299 cells and blotted against P-Tyr. 42

Figure 14: Inhibition of ABL in BCR-ABL positive cells does not change tyrosine phosphorylation of histones. K562 cells were treated with the ABL inhibitor Nilotinib for 24 hours followed by western blotting against P-Tyr. a) Western blot of whole cell extracts shows significant reduction of overall tyrosine phosphorylation. b) Western blot of histones shows no difference in tyrosine phosphorylation between cells treated with Nilotinib and DMSO. 43

Figure 15: Levels of histone tyrosine phosphorylation change during cell cycle progression. Karpas299 cells were synchronized by double thymidine block followed by acid extraction of histones every 2h after release. a) Flow cytometry analysis revealed that after 0h and 2h cells are in S phase, after 4h in G2 phase, after 6h in M phase, after 8h in G1 phase and after 10h a logarithmic distribution was detected. b) Western blot against P-Tyr indicates higher levels of histone Y phosphorylation during S phase. 44

Figure 16: ALK phosphorylates histones *in vitro*. *In vitro* Kinase assay with calf thymus histones (CTH) shows incorporation of ³²P ATP. Histones were phosphorylated by both ALK kinase immunoprecipitated from Karpas299 whole cell protein extracts (IP:ALK) and recombinant ALK (rALK). Phosphorylation of histones by recombinant ALK was drastically decreased by addition of the ALK inhibitor Crizotinib. 45

Figure 17: Histones H2B and H4 exhibit the highest levels of *in vitro* phosphorylation. *In vitro* kinase assay with single recombinant histones and recombinant ALK kinase reveals that all core histones, but not histone H1 can be phosphorylated by ALK *in vitro*, with H2B showing the highest level of phosphorylation followed by histone H4. 45

Figure 18: Histones H2B and H4 are phosphorylated by ALK immunoprecipitated from Karpas299 nuclear protein extracts. *In vitro* kinase assay reveals that ALK kinase precipitated from nuclear extracts is able to phosphorylate recombinant histones H2B and H4. Histone H2A shows a low level of phosphorylation that does not differ significantly from the assay with the IgG control..... 46

Table of tables

Table 1: Predicted ALK phosphorylation motifs in histones. PhosphoMotif Finder query for all human histone sequences yielded three possible ALK phosphorylation sites on histones H2B, H3 and H4. 46

Table 2: Tyrosine phosphorylation marks on histones in ALK+ ALCL cell lines and blood identified by mass spectrometry. Data were retrieved from the PhosphoSitePlus database. MW=molecular weight, kDa=kilo Dalton..... 47

1 ABSTRACT

Anaplastic large cell lymphoma (ALCL) is an aggressive T-cell non-Hodgkin lymphoma, which predominantly occurs in children and young adults. The ALK positive (ALK+) subcategory carries a translocation between the anaplastic large cell lymphoma kinase (*ALK*) locus and the nucleophosmin (*NPM*) gene. This translocation results in the aberrant expression of the NPM-ALK fusion protein, which constitutively phosphorylates a multitude of downstream targets, thereby activating numerous signaling pathways and driving the cell into tumorigenesis. Due to the heterodimerization of NPM-ALK with wildtype NPM, which functions as a nucleolar shuttleprotein, NPM-ALK is located in both cytoplasm and nucleus. However, all ALK targets that have been identified so far are of cytoplasmatic origin and little is known about the role of NPM-ALK in the nucleus. In this study, we aimed to identify nuclear tyrosine targets of the ALK kinase and inspired from the recent discovery of histone tyrosine phosphorylation, we specifically investigated the possibility that histones could be a target. We therefore analyzed the pattern of histone tyrosine phosphorylation in ALK+ ALCL cell lines and the effect of ALK inhibition on the phosphorylation levels. We furthermore tested the ability of ALK to phosphorylate histones *in vitro* and compared the data obtained from our studies to *in silico* data from different phosphorylation databases. We found that core histones in ALK+ ALCL cells exhibit high tyrosine phosphorylation levels, which can be reduced by treatment of the cells with an ALK inhibitor. Furthermore, a cell cycle dependent pattern of histone tyrosine phosphorylation was identified, showing that the tyrosine phosphorylation levels of selected histones are higher during S phase. Kinase assays revealed that ALK is able to phosphorylate histones *in vitro*, particularly histones H2B and H4. Consistently, *in silico* analysis identified possible ALK substrate motifs on these two histones, which were found actually phosphorylated in ALK+ ALCL cells by mass spectrometry. Taken together, our data from the ALK inhibitor treatments as well as the *in vitro* kinase assays and the *in silico* data provide strong evidence that ALK phosphorylates tyrosine residues on histones H2B and H4 in the nucleus of ALK+ ALCL cells.

2 ZUSAMMENFASSUNG

Das anaplastisch-großzellige Lymphom (ALCL) ist ein aggressives Non-Hodgkin T-Zell Lymphom, das gehäuft bei Kindern und jungen Erwachsenen auftritt. Die ALK positive (ALK+) Form ist durch die chromosomale Translokation zwischen anaplastic lymphoma kinase (*ALK*) und nucleophosmin (*NPM*) gekennzeichnet. Das dadurch entstehende Fusionsprotein NPM-ALK wird in den Zellen aberrant exprimiert und phosphoryliert durch die konstitutive Aktivierung der ALK Kinase zahlreiche Proteine. Dadurch wird eine Vielzahl von Signaltransduktionswegen angeschaltet und die Krebsentstehung beginnt. Im Gegensatz zu Wildtyp ALK ist NPM-ALK sowohl im Zytoplasma als auch im Zellkern lokalisiert, da es mit dem nukleolären Transportprotein NPM heterodimerisiert. Die Funktion von NPM-ALK im Zellkern ist jedoch weitgehend unerforscht und die bekannten Targets der ALK Kinase sind alle zytoplasmatischen Ursprungs. Das Ziel dieser Arbeit war die Identifikation von Kernproteinen, welche von der ALK Kinase an ihren Tyrosinresten phosphoryliert werden können. Nachdem in den letzten Jahren vermehrt Tyrosinphosphorylierungen an Histonen publiziert wurden, haben wir die Hypothese getestet, dass ALK im Zellkern aktiv ist und Histone phosphorylieren kann. Zuerst wurde die Tyrosinphosphorylierung an Histonen aus ALK+ ALCL Zelllinien charakterisiert und der Effekt von ALK Inhibierung untersucht. Weiters wurden Kinase assays durchgeführt, in denen die Fähigkeit der ALK Kinase, Histone *in vitro* zu phosphorylieren, analysiert wurde. Die aus diesen Experimenten gewonnenen Daten wurden schließlich mit Phosphorylierungsdaten aus verschiedenen Datenbanken verglichen. Die Analyse der Histone aus ALK+ ALCL Zellen zeigte, dass diese stark tyrosinphosphoryliert sind und dass der Grad der Phosphorylierung nach Behandlung der Zellen mit einem ALK Inhibitor abnimmt. Außerdem wurde eine Zellzyklus-abhängige Schwankung der Histon-Tyrosinphosphorylierung beobachtet, wobei die höchste Phosphorylierung während der S Phase auftrat. Kinase assays zeigten, dass ALK Histone *in vitro* phosphorylieren kann. Besonders auffällig war hier die Phosphorylierung von H2B und H4. In Übereinstimmung mit diesen Daten wurden bei der *in silico* Analyse mögliche ALK Substrat Motive auf diesen beiden Histonen gefunden. Diese wurden auch in einer Datenbank mit massenspektrometrischen Daten als tatsächlich phosphorylierte Tyrosinreste in ALK+ ALCL Zellen identifiziert. Zusammengefasst weisen unsere Ergebnisse und die

in silico Daten darauf hin, dass ALK im Zellkern von ALK+ ALCL Zellen aktiv ist und die Histone H2B und H4 an Tyrosinresten phosphorylieren kann.

3 INTRODUCTION

3.1 Anaplastic large cell lymphoma

Anaplastic large cell lymphoma (ALCL) represents a group of relatively rare, but aggressive non Hodgkin T-cell lymphoma that mostly affects children and young adults between 10 and 19 years of age with a slight male predominance. It was first described by Stein *et al.* in 1985, who showed the consistent expression of Ki-1 (later CD30) in tumors with large pleomorphic cells [1]. Systemic ALCL accounts for 2% to 8% of non-Hodgkin lymphomas in adults, rising to 10% to 15% in children [2]. According to the WHO's classification of tumors of hematopoietic and lymphoid tissues, systemic ALCL can be classified into two subcategories, ALK positive (ALK+) and ALK negative (ALK-) ALCL [3].

3.2 The role of NPM-ALK in ALK+ ALCL

ALK+ ALCL is characterized in up to 80% of cases by the fusion protein NPM-ALK, which results from a chromosomal translocation between the nucleophosmin gene (*NPM*) on chromosome 5q35 and the anaplastic large cell lymphoma kinase gene (*ALK*) on chromosome 2p23 [4, 5].

This leads to constitutive activation of the ALK kinase, which in the full-length protein is regulated by an extracellular ligand-binding domain [6, 7]. Structurally, NPM-ALK consists of a short part of the N-terminus of NPM containing the oligomerization domain and the C-terminal tyrosine kinase domain and intracellular tail of ALK [4] (Fig.1). The NPM oligomerization domain enables oligomerization of NPM-ALK, leading to tyrosine autophosphorylation and constitutive activation of the ALK kinase [6, 8].

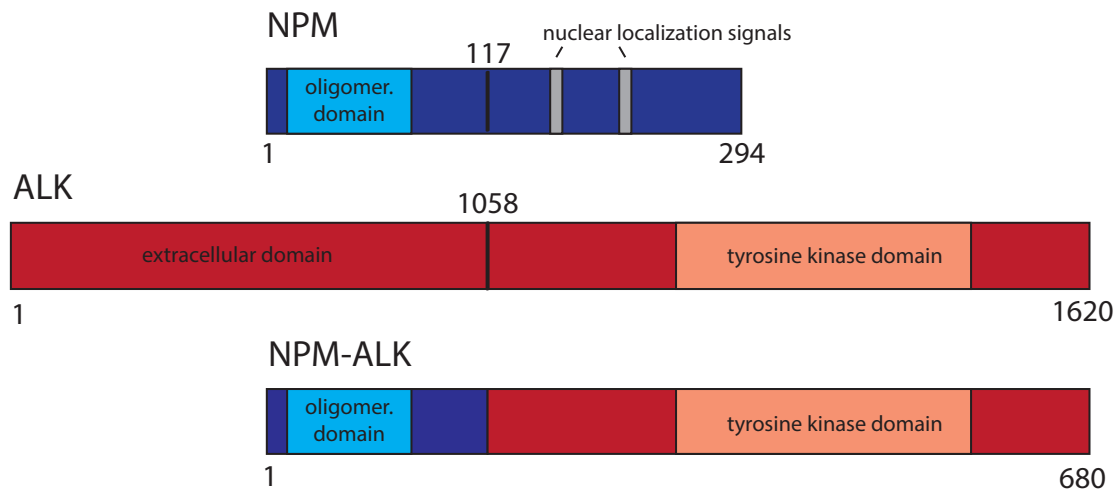


Figure 1: Schematic view of full-length ALK and NPM and the NPM-ALK fusion protein. In NPM-ALK, the extracellular region of ALK is lost and replaced by the N-terminal region of NPM containing the oligomerization domain, which enables the formation of heterodimers and activation of downstream signaling pathways.

3.2.1 Anaplastic lymphoma kinase (ALK)

ALK is a 210 kDa tyrosine kinase that together with leukocyte tyrosine kinase (LTK) forms a subfamily within the insulin growth factor receptor super family. Full-length ALK consists of an extracellular ligand-binding domain, a transmembrane domain and an intracellular tyrosine kinase domain. ALK expression is usually restricted to the nervous system, where it is highly expressed during embryogenesis, but only focally in the adult brain [6, 9]. The exact physiological function of ALK in mammals is unknown, although it might play a role in neuronal differentiation, indicated by its ability to induce neurite growth *in vitro* [10] and the function of its homologues in synapse formation in model organisms like *Cenorhabditis elegans* [11], *Drosophila melanogaster* [12] and the zebrafish *Danio rerio* [13]. In ALK+ ALCL, spatial and temporal restriction of ALK expression is lost, because it is driven by the promoter of the ubiquitously expressed binding partner NPM [14].

3.2.2 Nucleophosmin (NPM)

NPM1 is a highly conserved multifunctional protein, which acts as a molecular chaperone and exerts a role in shuttling of ribonucleoproteins between nucleolus and cytoplasm [15]. Furthermore it plays an important role in DNA repair, transcription and genomic stability [16]. The N-terminal domain of NPM1 provides a dimerization

domain that enables chimera autophosphorylation leading to constitutive activation of ALK and the firing of downstream signaling [8, 17].

3.2.3 ALK signaling

NPM-ALK constitutively activates a multitude of cellular signaling pathways including phospholipase Cγ (PLCγ), Janus kinase (JAK) – signal transducer and activator of transcription (STAT), MEK/ERK, mammalian target of rapamycin (mTOR) and phosphoinositide 3 kinase PI3K-AKT (Fig.2). Activation of these signaling cascades leads to increased cell growth and proliferation and resistance to apoptosis [18-20].

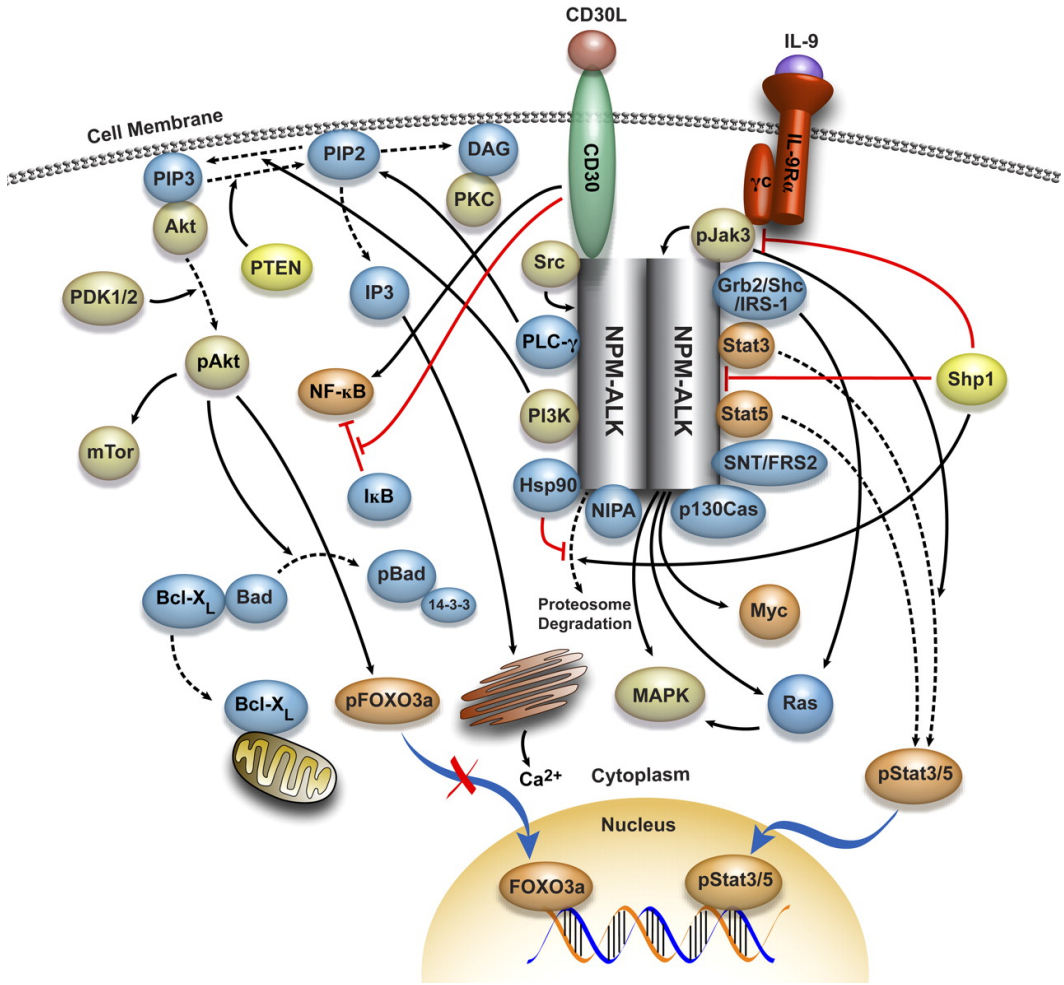


Figure 2: Molecular network interacting with NPM-ALK in ALK+ ALCL involving signaling pathways like JAK-STAT, PLC-γ, mTOR or Pi3K-AKT [2].

One of the key effector molecules of NPM-ALK mediated signaling in ALCL is STAT3 [21]. It is phosphorylated either directly by NPM-ALK or indirectly via JAK3 on its tyrosine residue Y705, which is crucial for STAT3 dimerization and activation [21, 22]. Active STAT3 migrates to the nucleus where it acts as a transcription factor

regulating expression of a multitude of genes, mostly involved in apoptosis, proliferation and cell cycle control [23-25]. The crucial role of STAT3 in ALCL has been demonstrated in a study by Chiarle et al. showing that STAT3 activation is required for NPM-ALK induced lymphagenesis and maintenance of the neoplastic phenotype [26]. Furthermore it has been shown that STAT3 functionally interacts with DNA methyltransferases leading to promoter hypermethylation and gene silencing [27]. One of the genes that have been shown to become silenced through STAT3-mediated hypermethylation is *SHP1*, encoding a tyrosine phosphatase that negatively regulates the STAT3 pathway [27-30].

3.3 General role of ALK in cancer

Although NPM-ALK is the most frequent translocation in ALCL occurring in up to 80% of cases [2, 3, 31], a plethora of other ALK translocation partners have been identified in ALCL, such as ring finger protein 213 (RNF213) [32], ATIC [33], TRK-fused gene (TFG) [34], moesin (MSN) [35], tropomyosin 3 (TPM3) [36] and TPM4 [37], myosin heavy chain 9 (MYH9) [38] and clathrin heavy chain (CLTC) [39].

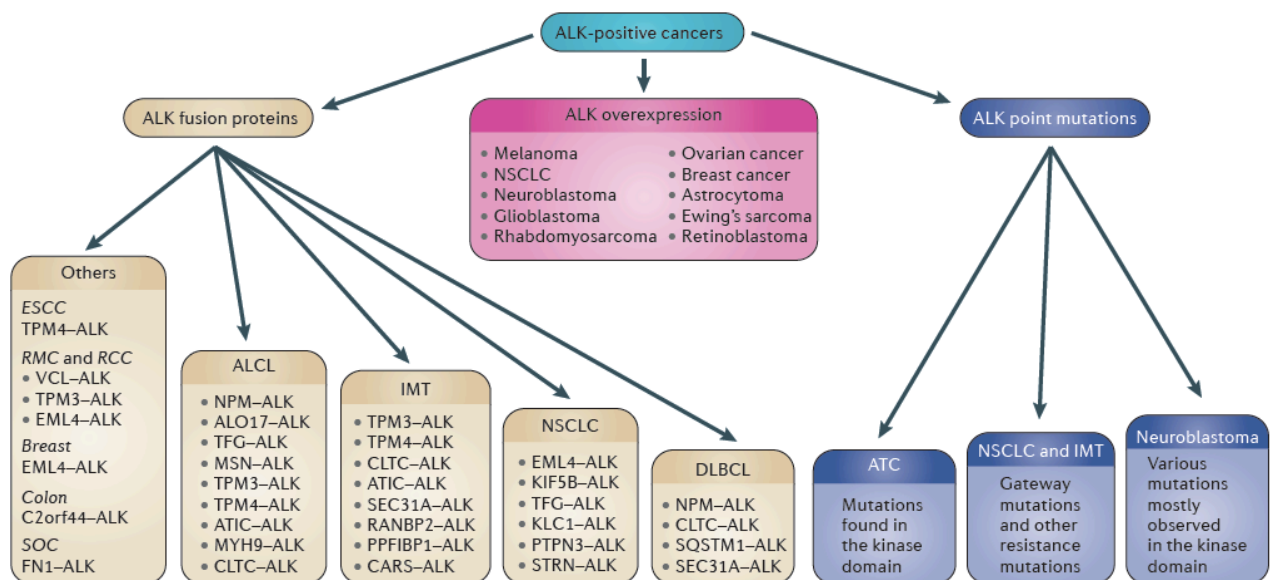


Figure 3: Overview of ALK in cancer. ALK fusion proteins (in beige) have been described in anaplastic large cell lymphoma (ALCL), inflammatory myofibroblastic tumor (IMT), non-small-cell lung cancer (NSCLC), diffuse large B cell lymphoma (DLBCL), oesophageal squamous cell carcinoma (ESCC), renal medulla carcinoma (RMC), renal cell carcinoma (RCC), breast cancer, colon carcinoma and serous ovarian carcinoma (SOC). ALK overexpression (pink) is yet not fully understood but has been reported in various cancer types. The third category are ALK point mutations (blue), which comprise both primary tumour-associated mutations and secondary mutations in Crizotinib-resistant patients. Secondary mutations have been described in NSCLC, IMT and anaplastic thyroid cancer (ATC). Primary point mutations are mainly found in neuroblastoma [40].

For reasons that are not fully understood yet, ALK seems to be a 'hotspot' for chromosomal translocations to a multitude of loci. So far, 22 different genes have been described as being translocated with ALK acting as oncogenic drivers not only in ALCL, but also in a number of both hematopoietic malignancies as well as solid tumors [18, 19]. Although ALK has so many different fusion partners, all chimeras share some common features. First, transcription of the respective ALK fusion protein is driven by the regulatory elements of the partner gene. Furthermore, localization within the cell is determined by the partner protein, causing ALK activity in both nucleus and cytoplasm depending on the translocation partner. Finally, the ALK partner protein is also responsible for dimerization and autophosphorylation of the fusion protein leading to constitutive activation of the ALK kinase domain [17, 40]. Furthermore, ALK activation in cancer does not only arise from translocations, but also through overexpression and mutation of full-length ALK [18, 40] (Fig.3).

3.4 Therapeutic approaches

The current standard therapy for both ALK+ and ALK- ALCL is doxorubicin-containing combination chemotherapy [41, 42], which in ALK+ ALCL is associated with an overall response rate of 90% and a 5-year survival rate of 70% [41]. Despite this relatively good prognosis, it is still desirable to develop alternative therapies for refractory or relapsed ALK+ lymphoma [43]. An alternative therapeutic approach is chemotherapy in combination with autologous stem cell transplantation for patients considered to be high risk [31, 44]. Animal model studies investigating the effect of immunotherapy or gene therapy in ALK+ ALCL yielded promising results [45, 46]. Christensen et al. also demonstrated strong inhibition of NPM-ALK and downstream signal transduction by the ALK inhibitor Crizotinib (PF-2341066) leading to induction of apoptosis and complete regression of ALCL in mouse xenograft studies [47]. Crizotinib is currently used in the therapy of non-small-cell lung cancer (NSCLC) involving a translocation between ALK and EML4 [48, 49]. Furthermore, it has been suggested that inhibition of the JUN and JUNB target platelet-derived growth factor receptor- β (PDGFRB) with Imatinib might be a possible therapeutic option for patients with relapsed ALK+ ALCL. It has been shown that Imatinib treatment of NPM-ALK transgenic mice significantly prolonged their survival

rates and Imatinib treatment of a patient with refractory late-stage ALK+ ALCL resulted in rapid, complete and sustained remission [50].

3.5 Histone modifications

Histones are highly alkaline eukaryotic proteins of fundamental importance for packaging of the DNA inside the nucleus [51]. Two molecules of each of the four core histones (H2A, H2B, H3 and H4) assemble to form an octameric histone core, around which 147 bp of DNA is wrapped 1.65 times in a super-helical turn. The resulting structure is the nucleosome, the basic repeating unit of chromatin [52]. Complementary to this classical role of histones as mere structural components of chromatin, a plethora of post-translational modifications on histones with crucial regulatory functions have been discovered over the past twenty years.

Each histone has a histone tail protruding from the nucleosome, which can be modified on its different amino acid residues. The major and most intensively studied core histone modifications that are currently known are acetylation and ubiquitylation on lysine residues, methylation on lysine and arginine residues and phosphorylation on serine and threonine residues [53]. These histone modifications can change the accessibility of the genetic information contained in the DNA, thereby regulating the expression of different genes [54].

3.6 Histone tyrosine phosphorylation

Phosphorylation on serine (S) and threonine (T) residues is involved in several cellular processes including apoptosis (H2B S10), mitosis (H3 S10 and S28), control of gene expression (H3 S10 and T11), meiosis and DNA damage response (H4 S1 and H2A.X S139) [53, 55-58]. Despite the long-known key role of protein tyrosine (Y) phosphorylation in signal transduction pathways regulating cellular activities like differentiation, cell growth and proliferation [59, 60], tyrosine phosphorylation of histones was not added to the list of post-translational histone modifications until 2009, when almost simultaneously five groups published papers describing histone tyrosine phosphorylation in both budding yeast and mammals [61-65]. Three of these papers identified histone tyrosine phosphorylation on the variant histone H2A.X, while the two others showed tyrosine residues on histone H3 to be phosphorylated. These histone marks have been associated with DNA damage response (H2A.X

Y142), histone turnover (H3 Y99) and chromatin structure and oncogenesis (H3 Y41). In 2012, another paper on histone tyrosine phosphorylation followed, describing phosphorylation of H2B on Y37, which plays a role in suppressing the expression of replication-dependent core histone genes [66] (Fig.4).

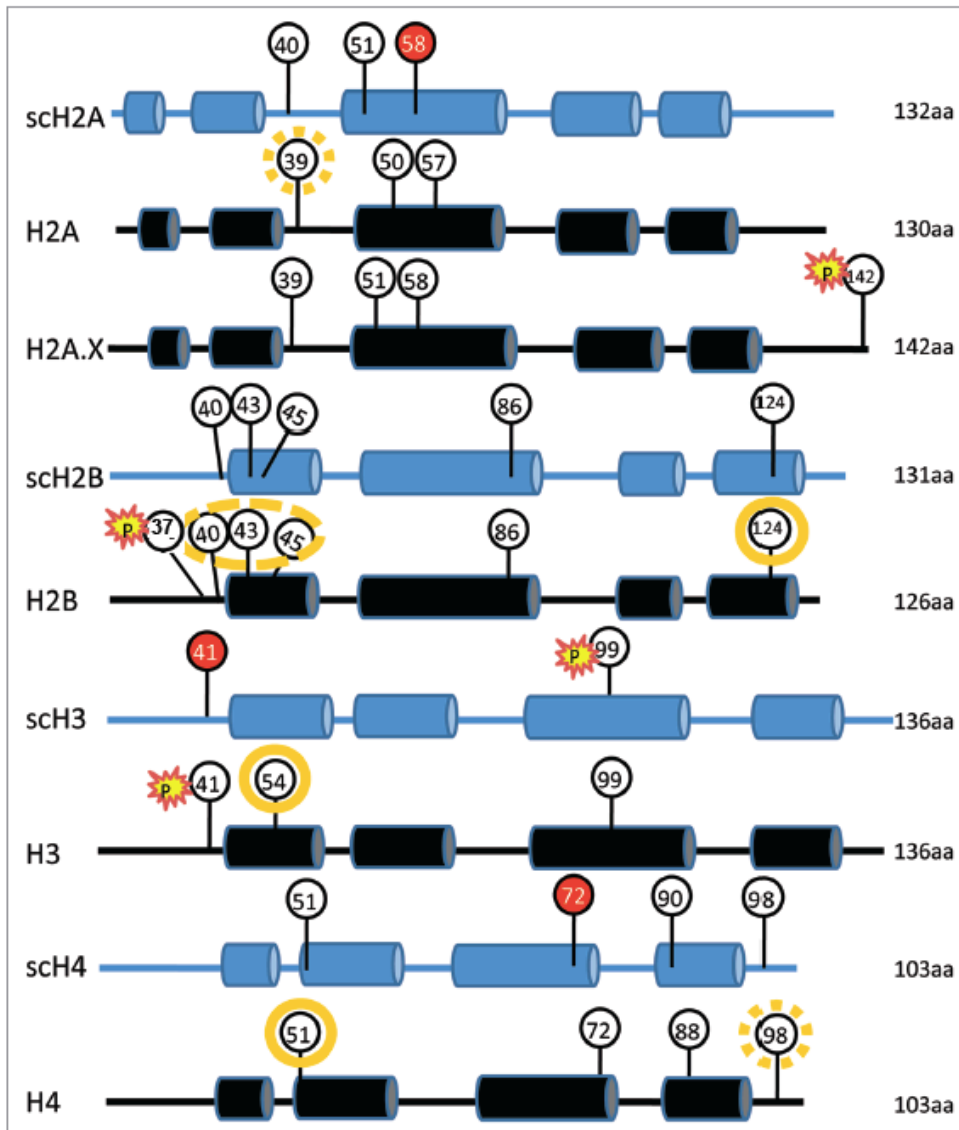


Figure 4: Overview of tyrosine residues in histones from budding yeast and mammals. The four yeast core histones are marked by the prefix “Sc” and denoted in blue. Mammalian histones are shown in black. The number of amino acid residues (aa) in each histone are noted on the right. The cylinders mark the location of α -helices. Tyrosine residues are shown as balloons. Red balloons mark the tyrosine residues essential for viability in budding yeast. Yellow explosion signs and a “P” mark tyrosine residues that have been shown to be phosphorylated *in vivo*. Tyrosines that are predicted to be accessible in the nucleosome and can therefore be potentially phosphorylated are indicated by a yellow circle. Solid lines indicate higher probability of phosphorylation, while dashed lines indicate lower probability. Modified after [67].

3.6.1 Tyrosine residues in core histones

The most conserved residues within the highly conserved histone proteins are tyrosines, pointing at a strong selective pressure that kept them unchanged during evolution [51]. Indeed, tyrosine residues on core histones are not only targets for phosphorylation, they are also implicated in maintenance of nucleosome structure via the formation of hydrogen bonds and ring-stacking interactions [68]. As mentioned above, in recent years a regulatory function has been added with the discovery of histone tyrosine phosphorylation.

3.6.2 Phosphorylation on H2A.X Y142 regulates DNA repair and apoptosis

The first histone tyrosine residue that was shown to become phosphorylated was Y142 on histone H2A.X. H2A.X is a variant histone that makes up approximately 10% of total H2A in the cell and plays a role in DNA repair [69]. It has been shown several years ago that H2A.X is phosphorylated on S139 as a result of double strand breaks (DSBs) mainly by ataxia telangiectasia mutated (ATM) kinase over large chromatin domains, thereby recruiting multiple DNA repair factors via recognition of the C-terminus of phospho-H2A.X (γ H2A.X) by Mediator of DNA damage checkpoint protein 1 (MDC1), resulting in the formation of repair complexes [70-73]. It had remained elusive how exactly the phosphorylation of γ H2A.X is regulated in response to DNA damage until Xiao et al. showed that Y142 is constitutively phosphorylated under normal physiological conditions and becomes dephosphorylated upon DNA damage. They further identified Williams-Beuren Syndrome transcription factor (WSTF), which is part of the WSTF-ISWI ATP-dependent chromatin-remodeling complex (WICH complex) as the factor carrying out this phosphorylation mark. Following DNA damage, WSTF dissociates from chromatin, leading to a decrease in Y142 phosphorylation, which in turn promotes maintenance of S139 phosphorylation and recruitment of MDC1 and other repair factors [62]. Two other groups independently described H2A.X Y142 phosphorylation and showed that this modification is regulated via dephosphorylation by EYA phosphatases [61, 63]. Cook et al. also showed that doubly phosphorylated H2A.X does not bind MDC1, indicating that Y142 dephosphorylation is a prerequisite for the accumulation of γ H2A.X. Instead, it was bound by c-Jun N-terminal protein kinase 1 (JNK1), a protein that can

induce apoptosis. This observation leads to the hypothesis that the phosphorylation status of Y142 could be crucial in determining cell fate after DNA damage [63, 74].

3.6.3 Tyrosine 41 on H3 is phosphorylated by JAK2 in hematopoietic cells

Dawson et al. showed that tyrosine 41 on histone H3 gets directly phosphorylated by JAK2 in human hematopoietic cell lines. They also demonstrated that H3 Y41 phosphorylation status modulates binding of heterochromatin protein 1 α (HP1 α) to histone H3 in a way that Y41 phosphorylation destabilizes HP1 α binding.

Furthermore, Dawson et al. showed that JAK2 inhibition leads to reduced expression of leukemia oncogene *LMO2*, probably due to the altered chromatin architecture resulting from increased HP1 α binding [65]. This means that on the contrary oncogenes like *LMO2* can be upregulated via JAK2 overexpression, H3 Y41 phosphorylation and loss of HP1 α binding, thereby promoting oncogenesis of hematopoietic cells (Fig.5).

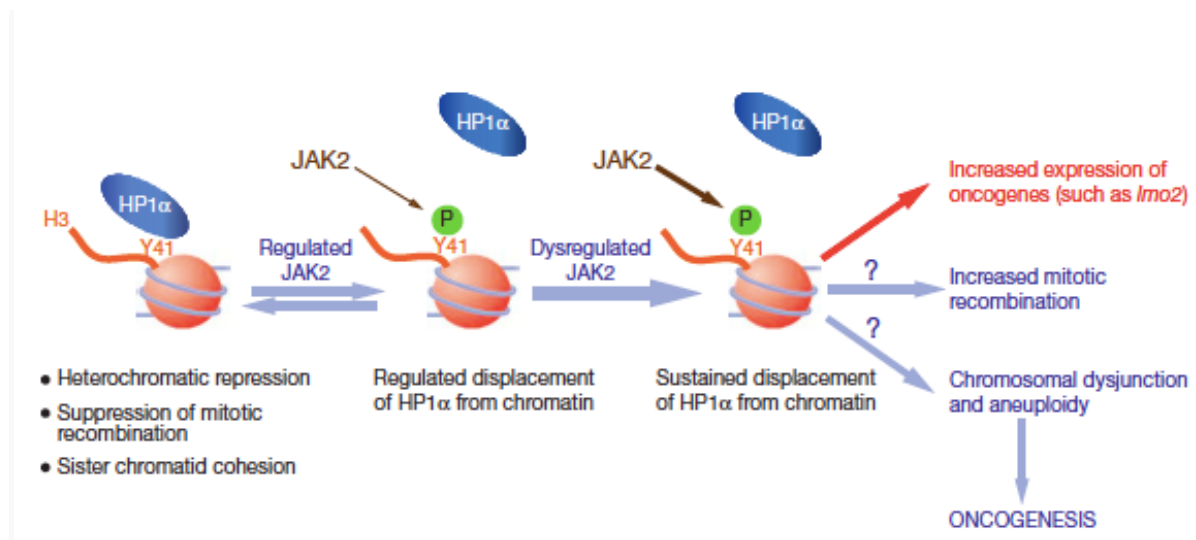


Figure 5: Model of JAK2 dependent phosphorylation of H3 Y41. In healthy cells JAK2 levels are tightly regulated, leading to regulated displacement of HP1 α from chromatin when H3 Y41 is phosphorylated and to heterochromatic repression, suppression of mitotic recombination and sister chromatid cohesion when H3 Y41 is not phosphorylated and HP1 α is bound to chromatin. Dysregulated JAK2 expression leads to sustained displacement of HP1 α from chromatin, which increases the expression of oncogenes like *LMO2* and probably also promotes mitotic recombination and chromosomal dysjunctions and aneuploidy, thereby driving the cell into oncogenesis [65].

In a subsequent study, Dawson et al. used chromatin immunoprecipitation coupled to massively parallel DNA sequencing (ChIP-seq) to analyze the genome-wide pattern of H3 Y41 phosphorylation in human erythroid leukemia cells. They found enrichment of H3Y41ph at three distinct sites: First, at a subset of active promoters, where it coincides with the active mark H3K4me3, second, at distal cis-regulatory elements,

where it overlaps with STAT5 binding and third, in transcribed regions of active, key tissue-specific hematopoietic genes [75].

3.6.4 Histone H3 Y99 phosphorylation regulates histone proteolysis in yeast

Phosphorylation of histone H3 on tyrosine 99 has been shown to play a crucial role in the regulation of histone proteolysis in yeast. The Y99 residue lays buried in the nucleosome at the interface of the H3-H4 heterodimer and can thus only be accessed when H3 is not bound to H4. Singh et al. showed that only this non-chromatin bound excess H3 is specifically targeted for degradation via phosphorylation on Y99 by radiation sensitive 53 (Rad53) kinase. In a nucleosomal context, the Y99 residue is inaccessible for Rad53, ensuring that only excess H3 becomes phosphorylated and subsequently ubiquitylated and degraded by the proteasome [64].

3.6.5 H2B Y37 phosphorylation suppresses expression of histone genes

The latest discovery in the field of histone tyrosine phosphorylation was made by Mahajan et al. in 2012, when they found that Y37 on histone H2B is phosphorylated during late S phase upstream of the histone gene cluster 1 (*Hist1*). They further identified WEE1 as the kinase responsible for this modification. Loss of WEE1 expression or inhibition of WEE1 abrogated H2BY37ph and led to an increase in histone transcription. This was shown both in yeast, where H2B Y40 is the equivalent of mammalian H2B Y37 as well as in mammalian cells. H2B Y37 phosphorylation inhibited binding of the transcriptional coactivator Nuclear Protein Ataxia-Telangiectasia Locus (NPAT) and RNA polymerase II and recruited the histone chaperone HIRA upstream of the *Hist1* cluster (Fig.6). These findings indicate that H2B Y37 phosphorylation by WEE1 kinase during late S phase inhibits transcription of multiple histone genes, thereby maintaining histone mRNA levels and lowering the burden on the histone mRNA turnover machinery [66].

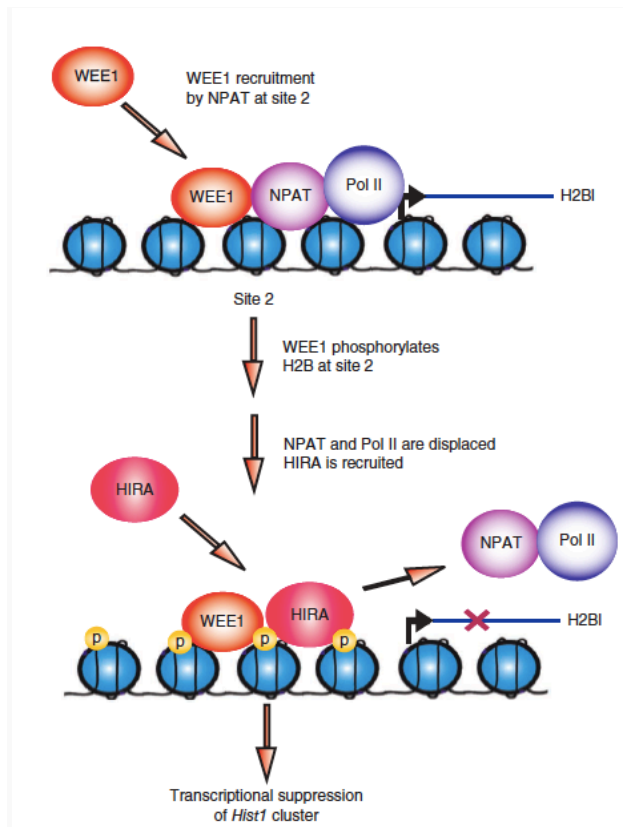


Figure 6: Model of H2B Y37 phosphorylation upstream of the histone gene cluster *Hist1*. WEE1 phosphorylates H2B at Y37 upstream of *Hist1*. NPAT is unable to recognize Y37-phosphorylated H2B and thus dissociates from chromatin. This in turn inhibits RNA polymerase II (Pol II) recruitment. Subsequently, HIRA is recruited to phosphorylated H2B Y37, preventing rebinding of NPAT and effectively suppressing histone mRNA synthesis [66].

3.6.6 Future perspectives

Among all histone modifications known to date, tyrosine phosphorylation is the most recently discovered one. It is now a field of extensive research and many important issues remain to be addressed. In future, major topics in ongoing research will be the exact regulation of those marks and the identification of kinases and phosphatases that are involved in the dynamics of histone tyrosine phosphorylation. Additionally, these studies could also provide information about how to target different players involved in the regulation of histone tyrosine phosphorylation in order to develop new therapies for various diseases. For example, small molecule inhibitors of EYA phosphatase might be useful to selectively modulate cancer cells to undergo apoptosis at lower doses of DNA damaging agents or radiation than currently used, thereby reducing the damage to healthy tissues. Another imaginable therapeutic approach targeting histone tyrosine phosphorylation would be inhibition of JAK2 or downstream signaling in certain hematopoietic malignancies, where JAK2

overexpression induces phosphorylation of H3 Y41, loss of HP1 α binding and subsequent upregulation of oncogenes [67].

Concerning the identification of new histone tyrosine phosphorylation marks, H3 Y54, H4 Y51 and H2B Y124 would be prime candidates for potential phosphorylation simply because of their accessibility and location within the nucleosome. Similar to H2A.X Y142 and H3 Y41, these relatively exposed tyrosine sites could be easily targeted by various regulatory factors. Additional tyrosines like H2A Y39, H2B Y40, -42 and -45 and H4 Y98 could also become accessible through chromatin remodeling and transcription induced nucleosome disruption [67, 76, 77] (Fig.4).

3.7 Project description and hypothesis

ALK+ ALCL is a complex disease involving the dysregulation of multiple signaling pathways. Although it is known that the cellular localization of the NPM-ALK fusion protein is determined by the NPM fusion partner, a chaperone that shuttles between nucleus and cytoplasm [15, 17], the pathways that have been identified so far to be dysregulated by NPM-ALK involved mainly cytoplasmic phosphorylation targets [18]. This led to the questions whether ALK is really present and active in the nucleus and if so, which nuclear proteins are targeted by the ALK tyrosine kinase. Since within the last few years there have been several reports of histone tyrosine phosphorylation as a new type of histone modification, also in the context of hematopoietic malignancies and oncogenesis [65], we speculated that histones might be a target. In order to test our hypothesis, the following experimental approaches were chosen:

- 1) In order to phosphorylate histones, ALK needs to be present and active in the nucleus. This was tested in ALK+ ALCL cell lines by immunofluorescence with ALK and phospho-ALK (P-ALK) antibodies as well as by cell fractionation into nuclear and cytoplasmic extracts followed by western blotting. If ALK is present in the nucleus, immunofluorescence with an ALK antibody will result in a nuclear staining pattern and ALK will also be detectable in the nuclear fraction on the blot. If the nuclear ALK is present in an active, phosphorylated form, immunofluorescence staining with the P-ALK antibody should also provide staining in the nucleus.

- 2) The second set of experiments served to characterize the pattern of histone tyrosine phosphorylation in ALK+ ALCL cells *in vivo* and to investigate its connection to ALK signaling. Therefore, histones were isolated from the ALK+ ALCL cell line Karpas299 and analyzed on western blots with an antibody against phospho-tyrosine (P-Tyr). In order to examine the effect of ALK signaling on histone tyrosine phosphorylation, Karpas299 cells were treated with the ALK inhibitor Crizotinib and phosphorylation levels of histones from these cells and untreated control cells were compared on western blot. In the event that ALK phosphorylates histones on tyrosine residues *in vivo*, a decrease in tyrosine phosphorylation levels after Crizotinib treatment would be expected. Furthermore, histones from Karpas299 cells were compared to those from peripheral blood mononuclear cells (PBMCs) of a healthy control, which should exhibit lower levels of tyrosine phosphorylation if ALK is able to phosphorylate histones. In order to investigate whether other tyrosine kinases like ABL have a similar function, the effect of ABL inhibition on tyrosine phosphorylation levels in BCR-ABL positive K562 cells was analyzed. Finally, cell synchronization using double thymidine block followed by flow cytometry analysis and western blotting was performed in order to assay histone tyrosine phosphorylation levels during cell cycle progression.
- 3) In order to test the ability of ALK to phosphorylate histones *in vitro*, kinase assays using radiolabeled ATP were performed. Assays were carried out with both recombinant and immunoprecipitated ALK kinase and calf thymus histones or recombinant single histones as substrates. If ALK is able to phosphorylate histones *in vitro*, it will transfer the ^{32}P to the respective histone and a band will be detectable on a phosphor screen. Addition of Crizotinib to the assay should result in ablation of phosphorylation.
- 4) Finally, the data obtained from our studies were compared to *in silico* data from phosphorylation databases. PhosphoMotif Finder was used to predict ALK substrate motifs in histone sequences based on sequence similarities to known substrate motifs from the literature. Furthermore, PhosphoSitePlus was used to browse through ALCL specific phosphorylation marks in mass spec data.

4 MATERIALS AND METHODS

4.1 Cell culture

Cell lines used in this study were the ALK+ cell lines Karpas299 and SU-DHL-1, ALK-Mac2a and the BCR-ABL positive cell line K562. K562 cells were obtained from Dr. Dagmar Stoiber-Sakaguchi, Ludwig Boltzmann Institute Vienna.

All cell lines were grown in RPMI (Gibco) supplemented with 10% FCS (Gibco) and 1% Penicillin/Streptomycin (Gibco) at 37°C and 5% CO₂. Cells were seeded at a concentration of 5x10⁵ cells per ml and split 1:3 every 2-3 days.

4.2 Inhibitor treatments

Cells were cultivated in RPMI supplemented with 1% Penicillin/Streptomycin and 20% FCS o/n in order to enhance phosphorylation by serum stimulation. Cells were then treated with the ALK inhibitor Crizotinib (DMSO stock, used at 1 µM for 5 h) or the ABL inhibitor Nilotinib (DMSO stock, used at 1 µM for 24 h). Control cells were incubated with the same volume DMSO.

4.3 Whole cell protein extraction

4.3.1 Buffers

4.3.1.1 HUNT buffer

20 mM Tris pH 8.0

100 mM NaCl

1 mM EDTA

0.5 % NP40

1 mM Na₃VO₄

1 x Protease inhibitor cocktail (Roche) added shortly before usage

4.3.2 Protocol

Cells were harvested and washed in 1x DPBS (Gibco). Pellets were resuspended in 2 x HUNT buffer and frozen in liquid nitrogen. After quick thawing at 37°C cells were again frozen in liquid nitrogen. Extracts were then allowed to thaw on ice and subsequently centrifuged for 10 minutes at 13.000 rpm at 4°C. Supernatants, representing whole cell protein extracts, were collected and protein concentration was determined by measuring A_{280} using a Nanodrop spectrophotometer.

4.4 Histone isolation

4.4.1 Buffers

4.4.1.1 *Lysis buffer*

10 mM Tris pH 6.5

50 mM $\text{Na}_2\text{S}_2\text{O}_5$

10 mM MgCl_2

1 % Triton X-100

8.6 % Sucrose

1 mM Na_3VO_4

1 x Protease Inhibitor cocktail (Roche) added shortly before usage

Adjust to pH 6.5

4.4.1.2 *Wash buffer*

10 mM Tris pH 7.4

13 mM Na_3EDTA

Adjust to pH 7.4

4.4.2 Protocol

Cells were harvested and washed in 1x DPBS (Gibco). Pellets were resuspended in 1 ml ice-cold lysis buffer and centrifuged at 1000 rpm at 4°C for 5 minutes. The supernatant was discarded and the pellet was washed 3 more times with 1 ml lysis buffer followed by one washing step with 1 ml washing buffer. The resulting pellet was resuspended in 100 µl 0.4N H₂SO₄ and incubated on ice for 1 hour followed by centrifugation at 12.000 rpm at 4°C for 10 minutes. Supernatants were collected and basic histones were precipitated with 10 volumes acetone at -20°C o/n. Histones were collected by centrifugation at 12.000 rpm at 4°C for 10 minutes. The supernatant was discarded and the pellets were air-dried at RT. Depending on the pellet size, histones were resuspended in 20-100µl milli-Q H₂O.

4.5 Preparation of nuclear and cytoplasmic protein extracts

4.5.1 Buffers

4.5.1.1 *Sucrose buffer*

0.32 M Sucrose

10 mM Tris/HCl pH 8.0

3 mM CaCl₂

2 mM Mg-Acetate

0.1 mM EDTA

0.5 % NP-40

1 mM Na₃VO₄

1 x Proteinase Inhibitor cocktail (Roche) added shortly before usage

4.5.1.2 *Low salt buffer*

20 mM HEPES pH 7.9

1.5 mM MgCl₂

20 mM KCl

0.2 mM EDTA

25 % Glycerol (v/v)

1 mM Na₃VO₄

1 x Proteinase Inhibitor cocktail (Roche) added shortly before usage

4.5.1.3 High salt buffer

20 mM HEPES pH 7.9

1.5 mM MgCl₂

800 mM KCl

0.2 mM EDTA

25 % Glycerol (v/v)

1 % NP-40

1 mM Na₃VO₄

1 x Proteinase Inhibitor cocktail (Roche) added shortly before usage

4.5.2 Protocol

Approximately 10⁷ cells were harvested and washed in cold 1 x DPBS (Gibco). PBS was aspirated and the cell pellet was resuspended in 100 µl sucrose buffer by gentle up and down pipetting. The released nuclei were then centrifuged at 2500 rpm for 5 minutes at 4°C. Supernatant, representing the cytoplasmic fraction, was transferred to a new tube and kept on ice until use. The nuclear pellet was washed three times with 1 ml sucrose buffer without NP-40. After centrifugation at 2500 rpm for 5 minutes at 4°C, the buffer was carefully removed and the pellet was resuspended in 40 µl low salt buffer by gentle finger vortexing. An equal volume of high salt buffer was added very slowly while mixing the lysate with the pipette tip. Nuclei were swollen 1.5 hours shaking at 4°C followed by centrifugation at 14000 rpm for 15 minutes at 4°C. The supernatant, representing the nuclear fraction, was transferred to a new tube. Both nuclear and cytoplasmic fractions were analysed by Western blotting.

For analysis of ALK expression in nucleus and cytoplasm, nuclear and cytoplasmic extracts were prepared using the NE-PER Nuclear and Cytoplasmic Extraction Kit (Pierce) according to the supplier's protocol.

4.6 Isolation of peripheral blood mononuclear cells (PBMCs)

Fresh blood was diluted 1:1 with PBS and layered over the same volume of lymphoprep medium. After centrifugation at 1000 rpm for 30 minutes without break, the middle layer, containing PBMCs, was transferred to a new tube, diluted with PBS and centrifuged at 1500 rpm for 5 minutes. The supernatant was discarded, PBMCs were washed one more time in PBS and the resulting pellet was shock-frozen in liquid nitrogen and stored at -80°C until further use.

4.7 Western Blotting

4.7.1 Buffers

4.7.1.1 *2 x DTT Loading dye*

100 mM Tris-HCl pH 6.8

200 mM DTT

4 % SDS

0.2 % Bromphenol blue

20 % Glycerol

4.7.1.2 *Electrophoresis buffer*

14.4 g Glycine

3 g Tris

1 g SDS

in 1 l H₂O

4.7.1.3 *Transfer buffer*

11.2 g Glycine

2.46 g Tris

200 ml Methanol
in 1 l H₂O

4.7.1.4 Ponceau red staining solution

0.1 % Ponceau red
5 % Acetic acid

4.7.1.5 10 x TBS (0.5 M)

60.5 g Tris
90 g NaCl
in 1 l H₂O
Adjust with HCl to pH 7.5
(TBS-T: 0.1% Tween-20)

4.7.1.6 Blocking solution

1 % PVP
5 % milk powder
0.01% Sodium azide

4.7.2 Protocol

Protein samples (60 µg total protein) in a volume of 10-20 µl were heated for 5 minutes in DTT loading dye at 95°C and separated on polyacrylamide gels (10% for protein extracts, 18% for histones) at 120V in electrophoresis buffer. Separated samples were blotted onto a nitrocellulose membrane in transfer buffer (200mA, 2 hours). Membranes were subsequently stained with Ponceau red to control transfer and equal loading of samples and blocked in blocking solution with shaking for one hour at RT. Incubation with primary antibody was performed o/n at 4°C using the recommended antibody dilutions in blocking solution. Membranes were washed 3 x 10 minutes in 1 x TBS-T and incubated with the appropriate secondary antibody

diluted 1:10 000 in TBS-T for 1 hour at RT. After 3 x 10 minute washing steps with 1 x TBS-T proteins were visualized with Amersham ECL plus Western blotting detection reagents in a LumiAnalyst imager (Roche).

4.7.3 SDS-polyacrylamide gels

The following recipes were used to cast 3 1 mm gels (6-7 ml resolving gel, 1-2 ml stacking gel per cassette).

Solution components	10%	18%	Stacking gel
H ₂ O	7.9 ml	2.6 ml	3.4 ml
30% acrylamide mix	6.7 ml	12 ml	0.83 ml
1.5 M Tris pH 8.8	5.0 ml	5 ml	–
1.0 M Tris pH 6.8	–	–	0.63 ml
10% SDS	0.2 ml	0.2 ml	0.05 ml
10% APS	0.2 ml	0.2 ml	0.05 ml
TEMED	0.008 ml	0.008 ml	0.005 ml

4.8 Immunofluorescence staining

Approximately 1 ml of cell suspension containing 1×10^6 cells was centrifuged onto a microscope slide in a Cytospin centrifuge at 600 rpm for 4 minutes. Cells were fixed with cold 4 % PFA in PBS for 10 minutes and permeabilized with 0.1 % Triton X-100 in PBS for 10 minutes. Subsequently, slides were washed 5 x 5 minutes with PBS and blocked with 10 mg/ml Endobulin S/D (Baxter, human IgG) diluted in PBS for 30 minutes. Slides were then washed with PBS for 10 minutes and incubated with primary antibody diluted in 2 % BSA in a humidified chamber at 4°C o/n. On the next day, slides were washed 3 x with PBS and incubated with secondary antibody diluted 1:1000 in 2 % BSA in a dark, humidified chamber at RT for one hour. After 3 more washes with PBS, cells were counterstained with DAPI diluted 1:50 000 in PBS for 5 minutes and mounted with GelTol. Slides were allowed to dry in the dark followed by imaging using a Zeiss Axio Observer Z1 laser scanning confocal microscope. Co-

Immunofluorescence staining with ALK1 and NPM antibodies was done by sequential staining with the two primary antibodies and secondary antibodies with different emission colours including a mouse block (ID Labs) for 1 hour at RT between the two stainings.

4.9 Immunoprecipitation

4.9.1 Buffers

4.9.1.1 *Washing buffer*

4.7 g Citric acid

9.2 g Na₂HPO₄

to 1 l with H₂O

Adjust pH to 5.0

4.9.1.2 *Elution buffer*

0.1 M Citric acid

Adjust pH to 2.0-3.0

4.9.1.3 *BS³ Conjugation buffer*

20 mM sodium phosphate

0.15 M NaCl

Adjust pH to 7.0-9.0

4.9.1.4 *BS³ Quenching buffer*

1 M Tris

Adjust pH to 7.5

4.9.1.5 *BS³ Crosslinking reagent*

5 mM BS³
in conjugation buffer

4.9.2 Protocol

50 µl Dynabeads Protein G (Invitrogen) per sample were washed 2 x in 500 µl washing buffer using a magnetic separator (Invitrogen) and resuspended in 100 µl washing buffer. For Ig capture, 5 µg antibody or IgG as a control were added and incubated with gentle mixing for 40 minutes at RT. Tubes were placed on the magnet, supernatant was discarded and samples were washed 3 x in washing buffer. For crosslinking, Ig-coupled beads were washed twice in 200 µl conjugation buffer and incubated in 250 µl BS³ crosslinking reagent with rotation for 30 minutes at RT. The crosslinking reaction was quenched by addition of 12.5 µl quenching buffer and incubation for 15 minutes at RT with rotation. Beads were washed with 100 µl elution buffer to elute non-crosslinked antibodies and subsequently washed 3 x with 200 µl PBST. 500-1000 µg protein sample diluted in PBS to a final volume of 500 µl was added to the Ig-coupled beads and incubated at 4°C with rotation o/n for immunoprecipitation. The next day, tubes were placed on the magnet, supernatant was discarded and beads were washed 3 x in 1 ml PBS. Beads were boiled in DTT loading dye for 10 minutes to release and denature immunoprecipitated proteins, which were subsequently analyzed by western blotting.

4.10 Cell synchronization by double thymidine block

Karpas299 cells were seeded at a density of at 2.5×10^5 cells per ml. 2 mM thymidine was added followed by incubation for 24 hours at 37°C. Cells were released by washing with PBS and addition of fresh medium for 12 hours. Cells were again blocked by addition of 2 mM thymidine for 24 hours followed by release in fresh medium. Aliquots of approximately 5×10^5 cells were fixed every 2 hours. Therefore cells were resuspended in 200 µl PBS and 800 µl ice-cold EtOH abs. was added dropwise while vortexing at low speed. As a control, unblocked Karpas299 cells were fixed. Fixed cells were stored at 4°C until PI staining and flow cytometry analysis.

4.11 PI staining and flow cytometry

Fixed cells were centrifuged at 1500 rpm for 10 minutes, EtOH was aspirated and cells were washed in PBS. For PI staining, 5×10^5 cells were resuspended in 100 μ l PBS, 500 μ l PI buffer (1% Na-citrate in PBS), 5 μ l RNase I, DNase-free (Roche), 0.5 μ l Triton X-100 and 5 μ l PI (Sigma) and incubated at 37°C in the dark for 30 minutes. Cell cycle analysis was done by flow cytometry using BD FACSDiva.

4.12 Kinase assays

4.12.1 Buffers

4.12.1.1 *2.5 x Standard assay buffer*

125 mM HEPES

7.5 mM MgCl₂

7.5 mM MnCl₂*4H₂O

7.5 μ M Na₄VO₃ (stock 50mM)

2.5 μ M DTT

Adjust pH to 7.5

4.12.1.2 *10 x Kinase dilution buffer*

500 mM HEPES

125 μ M PEG 20.000

10mM DTT

Adjust pH to 7.5

4.12.2 Protocol

The following reaction mixture was set up in a 1.5 ml tube:

- 10 μ l Standard assay buffer
- 2.5 μ l DMSO 10%
- 5 μ l calf thymus histones (Sigma) in milli-Q H₂O (2 μ g)/ 1 μ l single histones (NEB)(1 μ g)
- 5 μ l ALK kinase (ProQinase) (0.5 μ l stock (150ng) diluted in 1x kinase dilution buffer) / immunoprecipitated kinase on beads
- 0.5 μ l ³²P-ATP (5 μ Ci)
- H₂O to 25 μ l

The reaction mix was incubated at 30°C for 30 minutes, supplemented with 5 μ l DTT loading dye and boiled at 95°C for 5 minutes. Samples were run on PAA gels, which were then dried in a Biorad gel dryer 583 and exposed on a phosphor screen that was then imaged in a STORM 860 phosphor imager.

4.13 Antibodies

4.13.1 Primary Antibodies

Antibody	Company	Product number	Host	Dilution for WB	Dilution for IF
Phospho-Tyrosine (Y100)	Cell Signaling	#9411	mouse	1:2000	–
Phospho-STAT3 (Y705)	Cell signaling	#9145L	rabbit	1:2000	–
ALK1	DAKO	IR641/IS641	mouse	1:1000	1:100
Phospho-ALK (Y1604)	Cell signaling	#3341S	rabbit	1:1000	1:100
NPM	DAKO	IR652/IS652	mouse	1:1000	1:100
Hdac2	Cell signaling	#2540	rabbit	1:1000	–
GAPDH	Obtained from Prof. Kenner	–	rabbit	1:3000	–

4.13.2 Secondary Antibodies

4.13.2.1 *Western blot*

- Peroxidase-AffiniPure Rabbit Anti-Mouse IgG, Fcy (Jackson, 315-035-008)
- Peroxidase-AffiniPure F(ab')₂ Frag Goat Anti-Rabbit IgG (Jackson, 111-036-047)

4.13.2.2 *Immunofluorescence*

- Alexa Fluor 546 F(ab')₂ Fragment of Goat Anti-Mouse IgG (H+L) (Molecular Probes, A11018)
- Alexa Fluor 546 F(ab')₂ Fragment of Goat Anti-Rabbit IgG (H+L) (Molecular Probes, A11010)
- Alexa Fluor 488 F(ab')₂ Fragment of Goat Anti-Mouse IgG (H+L) (Molecular Probes, A11017)

4.14 Bioinformatic analysis

Kinase substrate motif prediction was performed using the online tool PhosphoMotif Finder [78]. It predicts substrate motifs of specific kinases based on sequence similarities to known substrate motifs from the literature.

Mass spec data of histones from ALK+ ALCL cell lines and blood samples were retrieved from the online phosphorylation database PhosphoSitePlus [79].

5 RESULTS

5.1 Identification of ALK in the nucleus

Immunofluorescence staining identified a significant amount of ALK in the nucleus of both ALK+ ALCL cell lines investigated, Karpas299 and SU-DHL-1. The specificity of the antibody was confirmed by the absence of any ALK signal in ALK- Mac2a cells (Fig. 7a). Subcellular fractionation of Karpas299 and SU-DHL-1 cells into nuclear and cytoplasmic protein extracts followed by western blotting also demonstrated ALK in the nucleus. HDAC2 as a nuclear marker and GAPDH as a cytoplasmic marker confirmed the purity of nuclear and cytoplasmic fractions. HDAC2 was restricted to the nuclear fraction and GAPDH was strongly enriched in the cytoplasmic fraction (Fig. 7b). Taken together, these results suggest a substantial proportion of ALK in the nucleus of ALK+ ALCL cells.

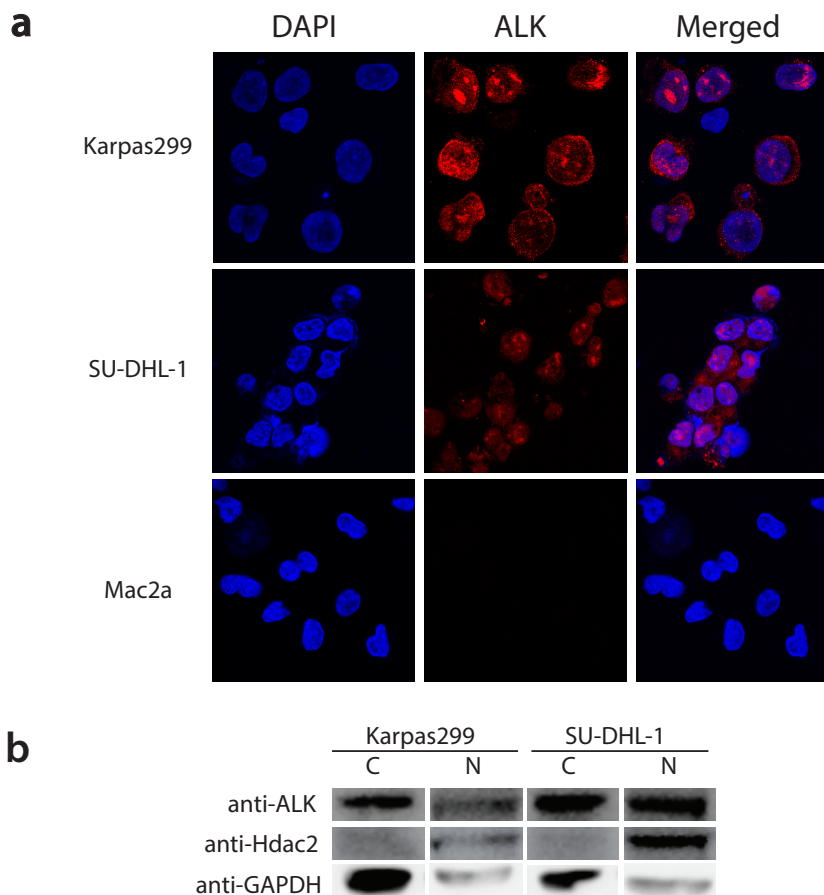


Figure 7: ALK is present in the nucleus of ALK+ ALCL cells. a) Confocal immunofluorescent images show nuclear ALK in Karpas299 and SU-DHL-1 cells. ALK- Mac2a cells do not show any ALK staining. b) Western blotting of cytoplasmic (C) and nuclear (N) extracts from Karpas299 and SU-DHL-1 cell lines identifies ALK in both cellular fractions, whereas Hdac2 is restricted to the nuclear compartment and GAPDH is enriched in the cytoplasmic fraction.

In order to assess whether the ALK kinase is active in the nucleus, immunofluorescence staining with an antibody against the active, phosphorylated form of ALK was performed. Phosphorylated ALK was detected in the nuclei of both ALK+ cell lines, Karpas299 and SU-DHL-1. ALK- Mac2a cells were used as a control and did not show any P-ALK staining. Thus, the ALK kinase seems to be present in an active form in the nuclei of ALK+ ALCL cells (Fig. 8).

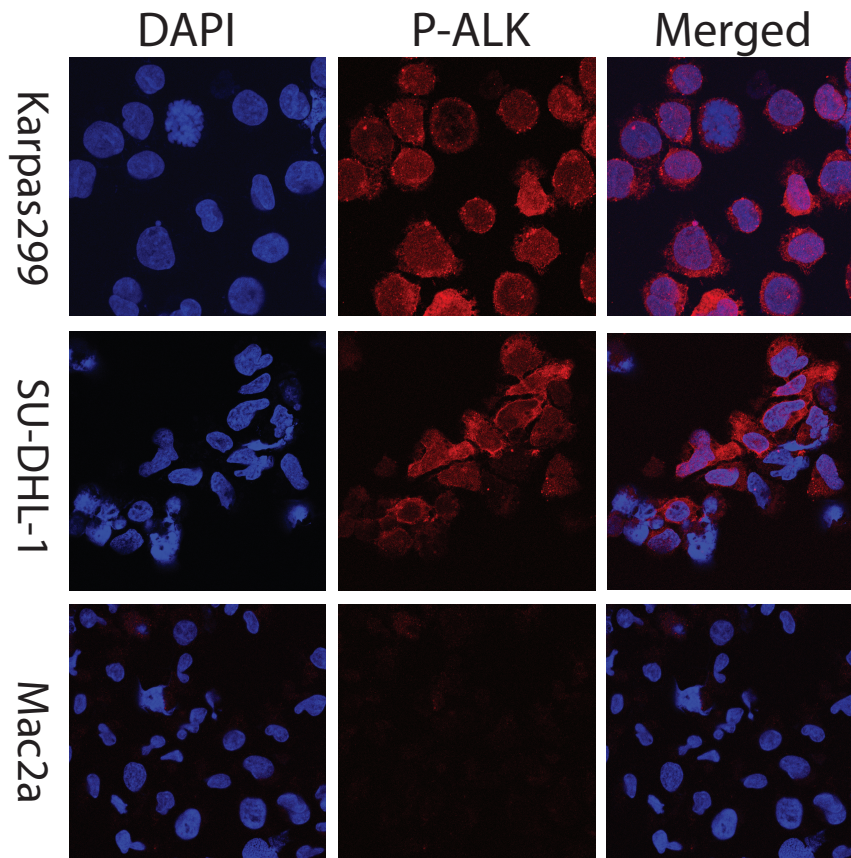


Figure 8: ALK is active in the nucleus of ALK+ ALCL cells. Immunofluorescence staining with an antibody against the active, phosphorylated form of ALK (P-ALK) detects P-ALK in the nuclei of both Karpas299 and SU-DHL-1 cells, but not in ALK- Mac2a cells.

Immunofluorescent confocal microscopy revealed a characteristic pattern of ALK in the nucleus with distinct spots of more intensive staining (Fig. 7a). To further analyze the significance of this pattern and to investigate the possibility of ALK being enriched in nucleoli, co-immunofluorescence with the nucleolar marker NPM was performed. In both Karpas299 and SU-DHL-1 cells, the spots observed in the ALK staining overlapped exactly with the NPM staining pattern, indicating co-localization of the two proteins in the nucleoli (Fig. 9).

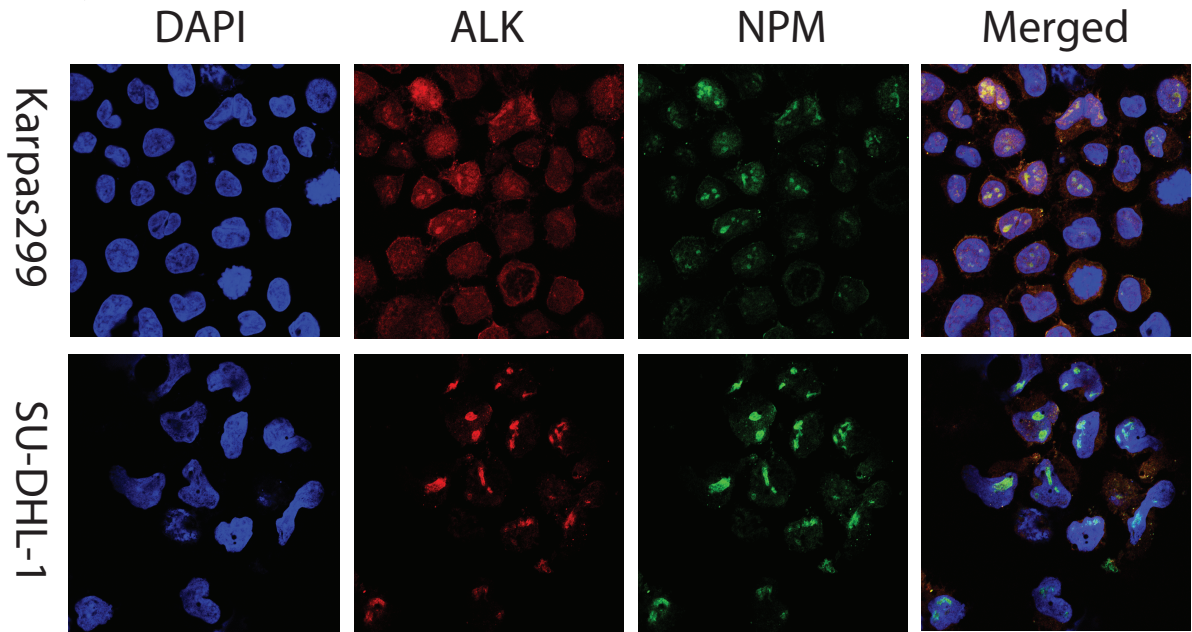


Figure 9: ALK is enriched in the nucleoli of ALK+ ALCL cells. Co-Immunofluorescence staining of ALK and the nucleolar protein nucleophosmin (NPM) reveals nucleolar localization of ALK in both Karpas299 and SU-DHL-1 cell lines indicated by overlapping staining patterns.

In order to check the possibility that co-localization of the two proteins is observed because the NPM antibody only detects the NPM-ALK transgene, immunofluorescence with NPM was also performed in ALK- Mac2a cells. Since the resulting pattern was similar to the ones observed in ALK+ cells, NPM seems to be a valid nucleolar marker (Fig. 10).

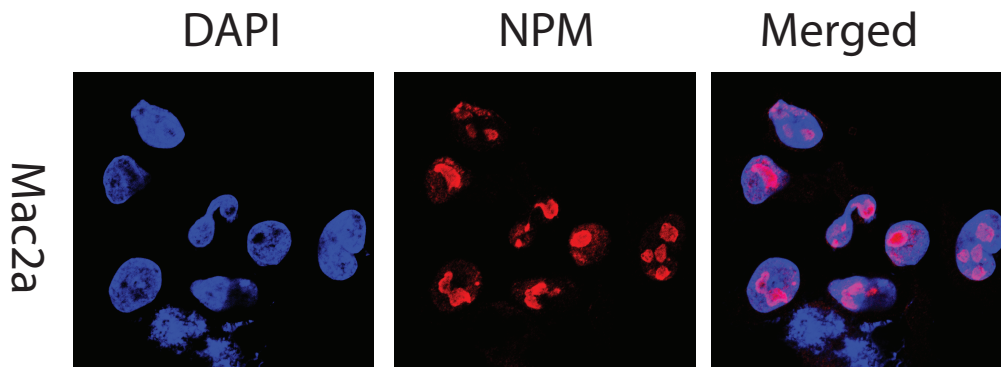


Figure 10: NPM marks nucleoli also in NPM- cells. NPM is a valid nucleolar marker, since it also detects NPM in the ALK- cell line Mac2a, where it shows a similar staining pattern as in ALK+ cells.

5.2 Characterization of histone tyrosine phosphorylation in ALK+ ALCL cells

Since both immunofluorescence and western blotting revealed a significant nuclear proportion of ALK in ALK+ ALCL cells, the next step was to investigate its role within the nucleus and to check for nuclear targets of the ALK kinase. As histones have recently been shown to become phosphorylated on a number of tyrosine residues by different tyrosine kinases, the next experiments focused on the possibility that histones could be a substrate.

Histones were extracted from Karpas299 cells, separated on 18% PAA gels and analyzed on western blots using an antibody against phosphorylated tyrosine (P-Tyr). Figure 11 shows that all core histones are tyrosine phosphorylated and that serum stimulation of the cells with 20% FCS added to the culture medium significantly enhances tyrosine phosphorylation levels.

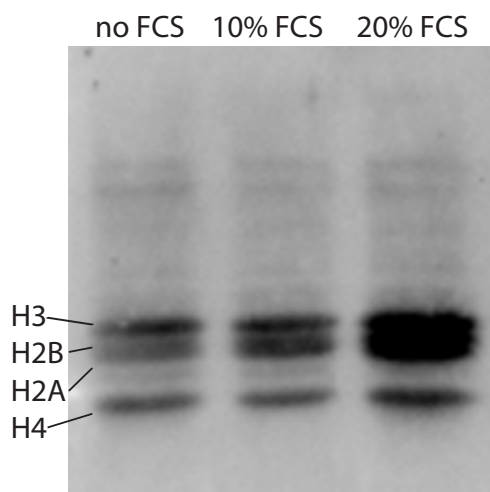


Figure 11: ALK+ ALCL cells show tyrosine phosphorylation on all core histones. Western blot of acid extracted histones from Karpas299 cells with antibody against P-Tyr shows tyrosine phosphorylation of all core histones. Tyrosine phosphorylation levels were increased by serum stimulation with 20% FCS (fetal calf serum).

Histone tyrosine phosphorylation levels were decreased significantly by treatment of serum-stimulated cells with the ALK inhibitor Crizotinib prior to histone isolation. Figure 12a shows that Crizotinib effectively inhibits phosphorylation of ALK and its downstream target STAT3. On the histone level, cells treated with Crizotinib display noticeably lower tyrosine phosphorylation than DMSO control cells for histones H3, H2B and H4. Nevertheless, also cells treated with the ALK inhibitor display relatively

high levels of histone tyrosine phosphorylation, indicating that ALK is not the only kinase involved (Fig. 12b).

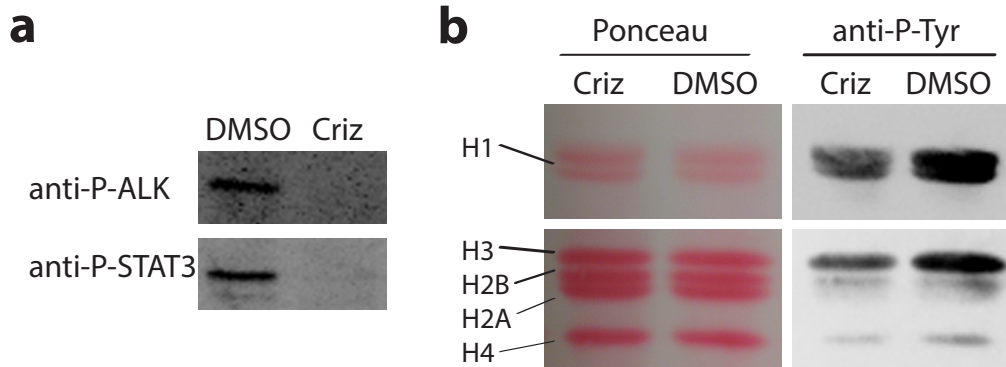


Figure 12: ALK inhibition reduces levels of histone tyrosine phosphorylation. a) Western blotting of whole cell protein extracts reveals that treatment of Karpas299 cells with Crizotinib inhibits phosphorylation of ALK and STAT3. b) Histone tyrosine phosphorylation is significantly reduced after Crizotinib treatment compared to the DMSO control.

Comparison between histones from ALK+ Karpas299 cells and peripheral blood mononuclear cells (PBMCs) from a healthy control female revealed higher tyrosine phosphorylation levels in Karpas299 cells, most pronounced for histones H3 and H2B (Fig. 13).

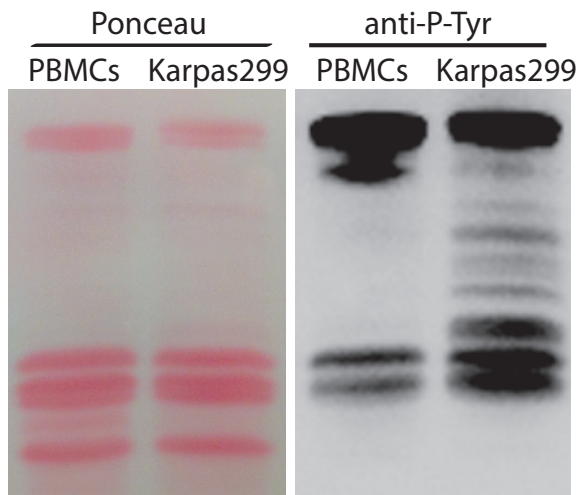


Figure 13: PBMCs from healthy controls show lower histone tyrosine phosphorylation levels than ALK+ ALCL cells. Histones were isolated from PBMCs of a healthy control and Karpas299 cells and blotted against P-Tyr.

In order to investigate, if the observed changes in histone tyrosine phosphorylation are specific for NPM-ALK+ cells or if it might be a common phenomenon in cells that harbor an oncogenic fusion protein involving a tyrosine kinase, histones from BCR-ABL+ K562 cells were analyzed. K562 cells were treated with the ABL inhibitor Nilotinib, which strongly decreased the overall tyrosine phosphorylation (Fig. 14a),

but did not alter histone phosphorylation levels compared to DMSO control cells (Fig. 14b). Thus, BCR-ABL activity does not have an influence on histone tyrosine phosphorylation and the observed differences following ALK inhibition seem to be specific for NPM-ALK+ cells.

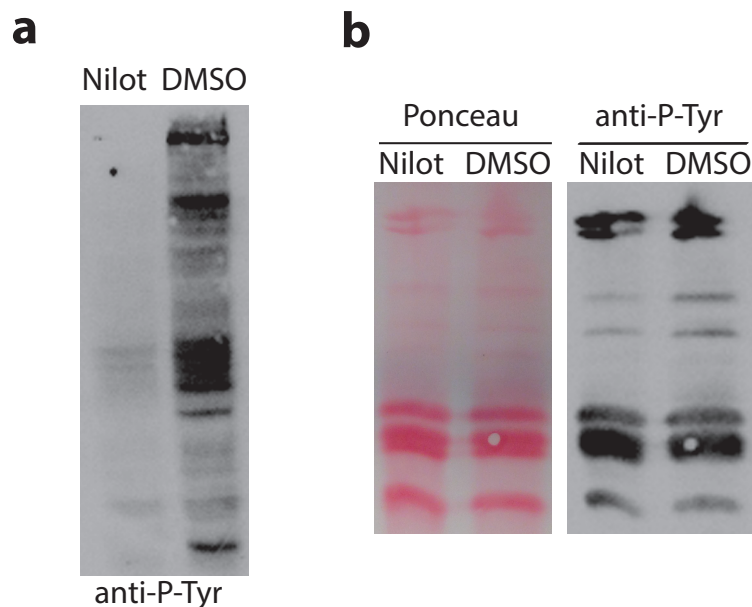


Figure 14: Inhibition of ABL in BCR-ABL positive cells does not change tyrosine phosphorylation of histones. K562 cells were treated with the ABL inhibitor Nilotinib for 24 hours followed by western blotting against P-Tyr. a) Western blot of whole cell extracts shows significant reduction of overall tyrosine phosphorylation. b) Western blot of histones shows no difference in tyrosine phosphorylation between cells treated with Nilotinib and DMSO.

In order to find out more about function and timing of the observed histone tyrosine phosphorylation during cell cycle progression, histones from different phases were analyzed. Thus, Karpas299 cells were synchronized by double thymidine block, which inhibits DNA synthesis and therefore arrests cells at the G1/S boundary. Cells were then released into fresh medium and aliquots of cells were collected every 2 hours for flow cytometry analysis and histone isolation. Flow cytometry analysis confirmed that the majority of cells was arrested at the G1/S boundary and progressed synchronously through the cell cycle to reach mid S phase by about 2 h, G2 phase by 4 h, G2/M phase by 6 h and G1 phase by 8 h after thymidine release. 10 h after release a more or less logarithmic distribution of cells was observed (Fig. 15a). Analysis of histones from those time points by western blot revealed higher levels of histone tyrosine phosphorylation at 0, 2 and 10 h after thymidine release. This indicates enrichment and a possible role of histone tyrosine phosphorylation during S phase (Fig. 15b).

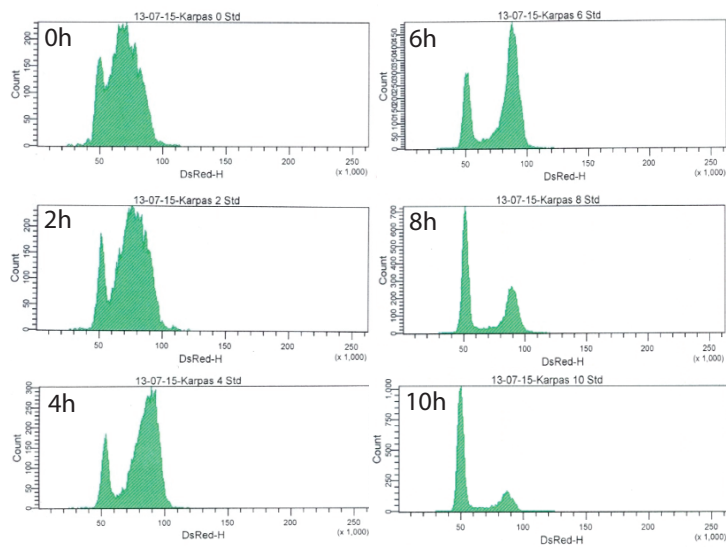
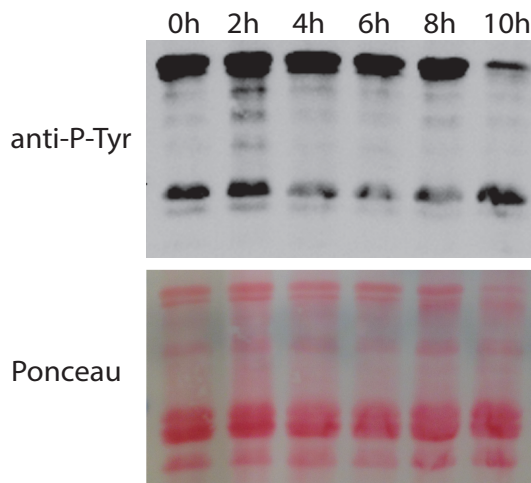
a**b**

Figure 15: Levels of histone tyrosine phosphorylation change during cell cycle progression. Karpas299 cells were synchronized by double thymidine block followed by acid extraction of histones every 2h after release. a) Flow cytometry analysis revealed that after 0h and 2h cells are in S phase, after 4h in G2 phase, after 6h in M phase, after 8h in G1 phase and after 10h a logarithmic distribution was detected. b) Western blot against P-Tyr indicates higher levels of histone Y phosphorylation during S phase.

5.3 *In vitro* kinase assays

To test whether ALK directly phosphorylates histones, *in vitro* kinase assays using ^{32}P -labeled ATP were performed. When ALK was incubated together with calf thymus histones (CTH), histones were phosphorylated and this phosphorylation was largely inhibited by treatment with the ALK inhibitor Crizotinib. The assay was done with both recombinant ALK and ALK immunoprecipitated from whole cell protein extracts from Karpas299 cells. In both cases, histones were phosphorylated by the

kinase, although the effect was much stronger when the recombinant kinase was used. Control reactions without ALK kinase did not result in any phosphorylation of histones (Fig. 16).

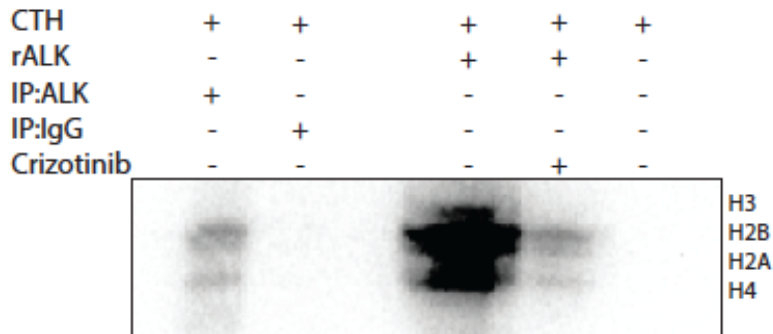


Figure 16: ALK phosphorylates histones *in vitro*. *In vitro* Kinase assay with calf thymus histones (CTH) shows incorporation of ³²P ATP. Histones were phosphorylated by both ALK kinase immunoprecipitated from Karpas299 whole cell protein extracts (IP:ALK) and recombinant ALK (rALK). Phosphorylation of histones by recombinant ALK was drastically decreased by addition of the ALK inhibitor Crizotinib.

An *in vitro* kinase assay using recombinant single histones as substrate and recombinant ALK kinase revealed that all core histones, but not histone H1 are phosphorylated by ALK *in vitro*. The highest level of phosphorylation was observed for histone H2B, followed by H4, H2A and H3 (Fig. 17).

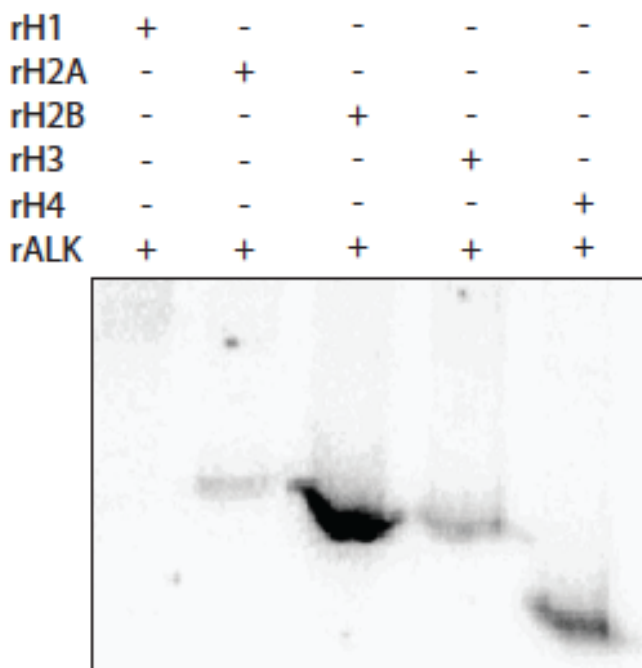


Figure 17: Histones H2B and H4 exhibit the highest levels of *in vitro* phosphorylation. *In vitro* kinase assay with single recombinant histones and recombinant ALK kinase reveals that all core histones, but not histone H1 can be phosphorylated by ALK *in vitro*, with H2B showing the highest level of phosphorylation followed by histone H4.

Since H2B, H4 and H2A were most strongly phosphorylated by recombinant ALK, we tested if these histones can also be phosphorylated *in vitro* by ALK immunoprecipitated from Karpas299 nuclear extracts. Figure 18 shows that this was the case for histones H2B and H4. For histone H2A a very low level of phosphorylation that did not differ significantly from the reaction with the IgG control was observed. Since the ALK kinase used in this assay was immunoprecipitated from nuclear protein extracts of Karpas299 cells it seems that ALK is really active in the nucleus of these ALK+ ALCL cells. According to the *in vitro* kinase assays, the main histone targets of ALK are histones H2B and H4.

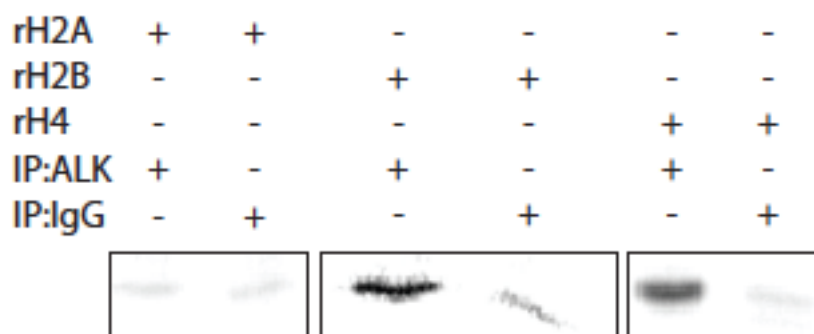


Figure 18: Histones H2B and H4 are phosphorylated by ALK immunoprecipitated from Karpas299 nuclear protein extracts. *In vitro* kinase assay reveals that ALK kinase precipitated from nuclear extracts is able to phosphorylate recombinant histones H2B and H4. Histone H2A shows a low level of phosphorylation that does not differ significantly from the assay with the IgG control.

5.4 *In silico* analysis of histone tyrosine phosphorylation

PhosphoMotif Finder was used to predict possible ALK kinase substrate motifs in histone sequences based on similarities to previously described phosphorylation motifs found in the literature. The query yielded three motifs in histones H2B (Y38-43), H3 (Y100-105) and H4 (Y86-89) (Tab. 1).

Table 1: Predicted ALK phosphorylation motifs in histones. PhosphoMotif Finder query for all human histone sequences yielded three possible ALK phosphorylation sites on histones H2B, H3 and H4.

Protein name	Position in query protein	Sequence in query protein	Corresponding motif described in the literature (phosphorylated residues in red)	Features of motif described in the literature
H2B	38 – 43	YSIYVY	pYXXXX[F/Y]	ALK kinase substrate motif
H3	100 – 105	YLVGLF	pYXXXX[F/Y]	ALK kinase substrate motif
H4	86 – 89	DVVY	[E/D]XxpY	ALK kinase substrate motif

Analysis of histone tyrosine phosphorylation sites in ALK+ ALCL cell lines and blood samples identified by mass spectrometry was done with the online tool PhosphoSitePlus. Tyrosine phosphorylation has been found on H2B and H4 in Karpas299 and TS cells, on H4 in SU-DHL-1 cells and on H2B and H4 in blood samples. On histone H2B, phosphorylation was identified on Y41 and Y43 and on histone H4 Y52 and Y89 were shown to be phosphorylated (Tab. 2).

Table 2: Tyrosine phosphorylation marks on histones in ALK+ ALCL cell lines and blood identified by mass spectrometry. Data were retrieved from the PhosphoSitePlus database. MW=molecular weight, kDa=kilo Dalton

Protein	Gene Symbol	MW (kDa)	Residue	Modification Type	cell line
H2B1C	HIST1H2BC	13,906	Y41-p	RKESYSVyyVYKVLKQ	Karpas299
H2B1D	HIST1H2BD	13,936	Y41-p	RKESYSVyyVYKVLKQ	Karpas299
H2B1H	HIST1H2BH	13,892	Y41-p	RKESYSVyyVYKVLKQ	Karpas299
H2B1K	HIST1H2BK	13,89	Y41-p	RKESYSVyyVYKVLKQ	Karpas299
H2B1L	HIST1H2BL	13,952	Y41-p	RKESYSVyyVYKVLKQ	Karpas299
H2B1M	HIST1H2BM	13,989	Y41-p	RKESYSVyyVYKVLKQ	Karpas299
H2B1N	HIST1H2BN	13,922	Y41-p	RKESYSVyyVYKVLKQ	Karpas299
H2B2F	HIST2H2BF	13,92	Y41-p	RKESYSVyyVYKVLKQ	Karpas299
H2BFS	H2BFS	13,944	Y41-p	RKESYSVyyVYKVLKQ	Karpas299
H4	HIST1H4A	11,367	Y52-p	KRISGLIyEETRGL	Karpas299
H4H4	HIST4H4	11,367	Y52-p	KRISGLIyEETRGL	Karpas299
H4	HIST1H4A	11,367	Y52-p	KRISGLIyEETRGL	SU-DHL-1
H4H4	HIST4H4	11,367	Y52-p	KRISGLIyEETRGL	SU-DHL-1
H2B	HIST1H2BB	13,95	Y41-p	RKESYSIyVYKVLKQ	TS
H2B1C	HIST1H2BC	13,906	Y41-p	RKESYSVyyVYKVLKQ	TS
H2B1D	HIST1H2BD	13,936	Y43-p	ESYSVYVyyKVLKQVH	TS
H2B1H	HIST1H2BH	13,892	Y41-p	RKESYSVyyVYKVLKQ	TS
H2B1K	HIST1H2BK	13,89	Y43-p	ESYSVYVyyKVLKQVH	TS
H2B1L	HIST1H2BL	13,952	Y41-p	RKESYSVyyVYKVLKQ	TS
H2B1M	HIST1H2BM	13,989	Y43-p	ESYSVYVyyKVLKQVH	TS
H2B1N	HIST1H2BN	13,922	Y41-p	RKESYSVyyVYKVLKQ	TS
H2B2E	HIST2H2BE	13,92	Y41-p	RKESYSIyVYKVLKQ	TS
H2B2F	HIST2H2BF	13,92	Y41-p	RKESYSVyyVYKVLKQ	TS
H2BFH	HIST1H2BO	13,906	Y41-p	RKESYSIyVYKVLKQ	TS
H2BFS	H2BFS	13,944	Y41-p	RKESYSVyyVYKVLKQ	TS
H4	HIST1H4A	11,367	Y89-p	VTAMDVVyALKRQGR	TS
H4H4	HIST4H4	11,367	Y52-p	KRISGLIyEETRGL	TS
H2B	HIST1H2BB	13,95	Y41-p	RKESYSIyVYKVLKQ	blood
H2B1C	HIST1H2BC	13,906	Y43-p	ESYSVYVyyKVLKQVH	blood
H2B1D	HIST1H2BD	13,936	Y41-p	RKESYSVyyVYKVLKQ	blood
H2B1H	HIST1H2BH	13,892	Y43-p	ESYSVYVyyKVLKQVH	blood
H2B1K	HIST1H2BK	13,89	Y41-p	RKESYSVyyVYKVLKQ	blood
H2B1L	HIST1H2BL	13,952	Y43-p	ESYSVYVyyKVLKQVH	blood
H2B1M	HIST1H2BM	13,989	Y41-p	RKESYSVyyVYKVLKQ	blood
H2B1N	HIST1H2BN	13,922	Y43-p	ESYSVYVyyKVLKQVH	blood
H2B2E	HIST2H2BE	13,92	Y41-p	RKESYSIyVYKVLKQ	blood
H2B2F	HIST2H2BF	13,92	Y41-p	RKESYSVyyVYKVLKQ	blood
H2BFH	HIST1H2BO	13,906	Y41-p	RKESYSIyVYKVLKQ	blood

H2BFS	H2BFS	13,944	Y41-p	RKESYSV _y VYKVLKQ	blood
H4	HIST1H4A	11,367	Y89-p	VTAMDVV _y ALKRQGR	blood
H4H4	HIST4H4	11,367	Y52-p	KRISGLI _y EETRGL	blood

6 DISCUSSION

The aim of this study was to confirm the nuclear localization of the NPM-ALK fusion protein and to investigate the effect of nuclear ALK kinase activity on histone tyrosine phosphorylation.

6.1 Identification of ALK in the nucleus

Concerning localization of NPM-ALK, both immunofluorescence and subcellular fractionation revealed the presence of the fusion protein in both nucleus and cytoplasm of ALK+ ALCL cells (Fig. 7). Immunofluorescence staining with an antibody against the phosphorylated, active form of ALK (P-ALK) also yielded cytoplasmic and nuclear staining, pointing at the fact that ALK is not only present, but also active in the nucleus (Fig. 8). Co-immunofluorescence with antibodies against ALK and NPM revealed co-localization of the two proteins in the nucleoli (Fig. 9). These findings are consistent with results from previous studies, where it was shown that despite the missing nuclear localization signals of NPM in the fusion gene (Fig. 1), NPM-ALK can be found in the nucleus of ALK+ ALCL cells [17, 80]. Bischof et al. provide evidence that this unexpected localization in the nuclear compartment is due to hetero-oligomerization of NPM-ALK and wild-type NPM [17]. Given that NPM functions as a shuttleprotein between nucleolus and cytoplasm and that it has been shown to homo-oligomerize in the cell, it seems plausible that NPM-ALK physically interacts with wild-type NPM via its oligomerization domain and is consequently shuttled into the nucleus [15, 81]. Although these data suggest that the nucleolar accumulation of NPM-ALK contributes directly to the pathogenesis of ALCL, it has been shown that the NPM domain and the nuclear localization of the fusion gene are not necessary for malignant cell transformation. Mason et al. have demonstrated that a fusion protein where the NPM portion of NPM-ALK is replaced by TPR (translocated promoter region) derived from the transforming TPR-MET protein, is localized exclusively in the cytoplasm, but nevertheless has nearly the same

transforming efficiency as NPM-ALK [80]. Furthermore, there are cases of ALCL that exhibit the same clinical and histopathological features like NPM-ALK-driven ALCL, carrying a divergent ALK translocation that leads to a different fusion protein, which is present only in the cytoplasm [9, 80, 82]. These data indicate that nucleolar localization of the ALK kinase is not a requisite for its oncogenic activity, probably because the constitutive activation of various cytoplasmatic signaling pathways is the main driver of ALK-induced oncogenesis. However, ALK is present and constitutively active in the nucleus, suggesting that it most likely phosphorylates nuclear proteins on their tyrosine residues. This may not be the driving force in tumorigenesis, but might very well contribute to the pathogenicity of ALK+ ALCL.

6.2 Characterization of histone tyrosine phosphorylation in ALK+ ALCL cells

We therefore investigated the possibility that histones might be targets of oncogenic ALK. Western blotting with an antibody against phosphorylated tyrosine revealed that in ALK+ ALCL cells all core histones are tyrosine phosphorylated. Serum stimulation leads to an increase in phosphorylation levels, probably due to the upregulation of signaling pathways (Fig. 11). Treatment of ALK+ ALCL cells with the ALK inhibitor Crizotinib completely inhibited the phosphorylation of ALK and its major downstream target STAT3, pointing at a very efficient inhibition of ALK activity (Fig. 12a). Tyrosine phosphorylation levels of all histones were significantly decreased after Crizotinib treatment. The effect was most pronounced for histones H1 and H3 (Fig. 12b). Comparison between histones from ALK+ ALCL cells and PBMCs from a healthy control revealed higher levels of tyrosine phosphorylation on H1, H3 and H2B in the ALK+ cells (Fig. 13). Taken together, these findings indicate that ALK either phosphorylates histones directly or via downstream signaling activates other tyrosine kinases, which in turn are able to phosphorylate histones. Nevertheless, the relatively high levels of histone tyrosine phosphorylation in Crizotinib treated samples indicate that ALK is not the only tyrosine kinase involved in histone phosphorylation in ALK+ ALCL cells.

In order to investigate the tyrosine phosphorylation of histones in another cancer harboring an oncogenic fusion protein that involves a tyrosine kinase, histones from BCR-ABL+ K562 cells were analyzed. Although treatment with the ABL inhibitor

Nilotinib resulted in a drastic global decrease in tyrosine phosphorylation (Fig. 14a), histones were not affected by the treatment and displayed similar tyrosine phosphorylation levels in Nilotinib treated and untreated cells (Fig. 14b). These results are in accordance with the mainly cytoplasmic subcellular localization of BCR-ABL [83] and indicate that the change in histone tyrosine phosphorylation after Crizotinib treatment in ALK+ cells is a specific effect resulting from the nuclear activity of NPM-ALK in these cells.

Cell cycle analysis revealed higher levels of histone tyrosine phosphorylation during S phase. This was most prominently observed on histone H3, although imaging of the western blot at longer exposure times unveiled that also H2B and H4 are phosphorylated more intensively during S phase. It remains to be clarified whether these histone tyrosine phosphorylation marks play a role during replication or histone deposition during S-phase and whether the cell-cycle dependent differences are due to ALK induced modifications or other histone tyrosine phosphorylation marks. The increased H3 tyrosine phosphorylation during S phase might represent H3Y41ph, which has been previously described as an activating histone mark that leads to dissociation of HP1 α from chromatin [65, 75]. Although this histone modification has so far only been identified as a positive regulator of transcription [75], it might also be involved in displacement of HP1 α during replication to enable proper binding and function of the DNA replication machinery. A similar mechanism of HP1 α displacement caused by H3S10ph during mitosis has been identified previously [84]. Although equal amounts of protein were loaded and confirmed by Ponceau S staining, the observed differences might simply result from the higher abundance of histones during S phase [85]. Despite the fact that the observed fluctuations in histone tyrosine phosphorylation levels during cell cycle progression display a highly interesting finding, further studies will be needed to investigate the exact identity and function of these histone marks.

6.3 *In vitro* kinase assays

The ability of ALK to phosphorylate histones *in vitro* was tested in kinase assays using ³²P-labeled ATP as a radioactive marker. When calf thymus histones were used as a substrate, all core histones were phosphorylated by both recombinant and immunoprecipitated ALK, although the signal was much stronger when recombinant

ALK was used. This is probably due to the higher amount of recombinant kinase used in the assay. The negative controls without ALK kinase did not yield any signal and the addition of Crizotinib to the assay significantly reduced the phosphorylation levels of all histones (Fig. 16), indicating that the observed phosphorylation was specifically induced by the ALK kinase. Kinase assays with recombinant ALK and recombinant histones revealed that all core histones, but not H1 can be phosphorylated by ALK. The highest phosphorylation level was detected for histone H2B, followed by H4, H2A and H3 (Fig. 17). H2B and H4 were also phosphorylated by ALK immunoprecipitated from nuclear extracts of Karpas299 cells (Fig. 18), adding weight to the argument that ALK is not only present but also active in the nucleus of these ALK+ cells. The phosphorylation levels of the respective single histones correspond to the results from the assays where calf thymus histones were used as substrates, although in these assays the individual histones were quite difficult to distinguish because of their similar molecular weights. Taken together, these results show that ALK is able to phosphorylate histones *in vitro*, in particular histones H2B and H4, which seem to be the main targets.

6.4 *In silico* analysis of histone tyrosine phosphorylation

Three possible ALK substrate motifs in histones were predicted based on sequence similarities to known ALK substrates using PhosphoMotif Finder. The predicted motifs are H2B Y38-43, H3 Y100-105 and H4 Y86-89 (Tab. 1). All three motifs had been extracted from a large set of mass spectrometry data that were generated with the use of an antibody against phospho-tyrosine to enrich for phosphorylated tyrosine residues in ALK+ Jurkat cells [86, 87].

Furthermore, we used PhosphoSitePlus to search for histone tyrosine phosphorylation marks that had been identified by mass spectrometry analysis. The query yielded a list of tyrosine phosphorylation sites identified in Karpas299, TS and SU-DHL-1 cells and blood samples that are all located on histones H2B and H4. On histone H2B, phosphorylation was identified on Y41 and Y43 and on histone H4 Y52 and Y89 were found to be phosphorylated (Tab. 2). Three out of these four sites had also been identified by the ALK substrate motif search, pointing at the reliability of the results from both databases and strengthening the argument that H2B and H4 are nuclear targets of the ALK kinase in ALK+ ALCL cells.

6.5 Conclusion

The aim of this study was to determine the exact subcellular localization of the NPM-ALK fusion protein in ALK+ ALCL cells and to investigate the possibility that histones could represent a nuclear phosphorylation target of the ALK tyrosine kinase.

Concerning the localization of ALK within the cell, we identified the fusion protein in both cytoplasm and nucleus. Nuclear staining showed a characteristic pattern, indicating that NPM-ALK is enriched in nucleoli. This finding corresponds to the hypothesis that NPM-ALK heterodimerizes with wildtype NPM, which serves as a nucleolar shuttleprotein and transports the fusion protein to the nucleolus [17]. Furthermore, we showed the nuclear occurrence of phosphorylated ALK, indicating that ALK is not only present, but also active in the nucleus. Although it has been shown that nuclear localization is not essential for the oncogenic activity of the ALK kinase [80], we speculated that given its constitutive nuclear activity, it will probably also target nuclear proteins. Since histones constitute highly abundant nuclear proteins and have recently been shown to become phosphorylated on various tyrosine residues [67], we examined the possibility that they could be a substrate of the ALK kinase. Western blotting with an antibody against phosphorylated tyrosine revealed that all core histones in ALK+ ALCL cells are tyrosine phosphorylated and that the phosphorylation levels are decreased after treatment of the cells with the ALK inhibitor Crizotinib. These results indicate that ALK is involved in the tyrosine phosphorylation of histones, either directly or indirectly via downstream activation of other tyrosine kinases. Analysis of histone tyrosine phosphorylation during cell cycle progression revealed higher phosphorylation levels during S phase, suggesting a possible role of histone tyrosine phosphorylation marks during replication.

In vitro kinase assays demonstrated that ALK is able to phosphorylate all core histones *in vitro*, although the strongest phosphorylation levels were detected for H2B and H4. Consistently, *in silico* analysis of possible ALK substrate motifs in histones revealed three motifs located in histones H2B, H3 and H4. The query for histone tyrosine phosphorylation sites that have been identified in ALK+ ALCL cells by mass spectrometry yielded phosphorylation marks on H2B and H4. The phosphorylated residues overlapped with the predicted motifs from the PhosphoMotif Finder query. Taken together, the *in vitro* and *in silico* data provide convincing evidence that ALK phosphorylates tyrosine residues on histones H2B and H4 in the nucleus of ALK+ ALCL cells. The intensive tyrosine phosphorylation of histone H3

that we observed on western blots of histones from ALK+ ALCL cell lines is probably induced by another tyrosine kinase. As the H3 tyrosine phosphorylation level was also decreased after Crizotinib treatment, the responsible kinase might be a downstream target of ALK signaling. Since H3Y41 has been shown to become phosphorylated by JAK2, which constitutes a downstream target of ALK, the observed changes in H3 phosphorylation after ALK inhibition might result from this JAK2-mediated histone modification.

6.6 Outlook

The data in this thesis provide evidence that histones become phosphorylated on their tyrosine residues by nuclear ALK kinase activity in ALK+ ALCL cells. Further studies should address the exact residues where these phosphorylation marks are located. This could be done by mass spectrometry analysis of histones from ALK+ ALCL cells cultured in the presence and absence of an ALK inhibitor, respectively. By comparing the data from these two samples, ALK dependent phosphorylation marks could be identified. Once it is clear which tyrosine residues on which histones are affected, modification-specific antibodies should be generated, allowing a more precise characterization of the respective modifications. Chromatin immunoprecipitation coupled to massively parallel DNA sequencing could be done to identify the genomic regions where the tyrosine phosphorylation marks are located, thereby revealing more information about their possible function. Moreover, the cell cycle dependent fluctuation in tyrosine phosphorylation levels could be further analyzed in order to determine the possible role of histone tyrosine phosphorylation during DNA replication. This could as well be facilitated by the availability of modification-specific antibodies.

7 REFERENCES

1. Stein, H., et al., *The expression of the Hodgkin's disease associated antigen Ki-1 in reactive and neoplastic lymphoid tissue: evidence that Reed-Sternberg cells and histiocytic malignancies are derived from activated lymphoid cells.* Blood, 1985. **66**(4): p. 848-58.
2. Amin, H.M. and R. Lai, *Pathobiology of ALK+ anaplastic large-cell lymphoma.* Blood, 2007. **110**(7): p. 2259-67.
3. Swerdlow, S.H.e.a., *WHO Classification of Tumours of Hematopoietic and Lymphoid Tissues.* 2008, Lyon: IARC.
4. Morris, S.W., et al., *Fusion of a kinase gene, ALK, to a nucleolar protein gene, NPM, in non-Hodgkin's lymphoma.* Science, 1994. **263**(5151): p. 1281-4.
5. Shiota, M., et al., *Anaplastic large cell lymphomas expressing the novel chimeric protein p80NPM/ALK: a distinct clinicopathologic entity.* Blood, 1995. **86**(5): p. 1954-60.
6. Iwahara, T., et al., *Molecular characterization of ALK, a receptor tyrosine kinase expressed specifically in the nervous system.* Oncogene, 1997. **14**(4): p. 439-49.
7. Morris, S.W., et al., *ALK, the chromosome 2 gene locus altered by the t(2;5) in non-Hodgkin's lymphoma, encodes a novel neural receptor tyrosine kinase that is highly related to leukocyte tyrosine kinase (LTK).* Oncogene, 1997. **14**(18): p. 2175-88.
8. Fujimoto, J., et al., *Characterization of the transforming activity of p80, a hyperphosphorylated protein in a Ki-1 lymphoma cell line with chromosomal translocation t(2;5).* Proc Natl Acad Sci U S A, 1996. **93**(9): p. 4181-6.
9. Pulford, K., et al., *Detection of anaplastic lymphoma kinase (ALK) and nucleolar protein nucleophosmin (NPM)-ALK proteins in normal and neoplastic cells with the monoclonal antibody ALK1.* Blood, 1997. **89**(4): p. 1394-404.
10. Souttou, B., et al., *Activation of anaplastic lymphoma kinase receptor tyrosine kinase induces neuronal differentiation through the mitogen-activated protein kinase pathway.* J Biol Chem, 2001. **276**(12): p. 9526-31.
11. Liao, E.H., et al., *An SCF-like ubiquitin ligase complex that controls presynaptic differentiation.* Nature, 2004. **430**(6997): p. 345-50.
12. Bazigou, E., et al., *Anterograde Jelly belly and Alk receptor tyrosine kinase signaling mediates retinal axon targeting in Drosophila.* Cell, 2007. **128**(5): p. 961-75.
13. Yao, S., et al., *Anaplastic lymphoma kinase is required for neurogenesis in the developing central nervous system of zebrafish.* PLoS One, 2013. **8**(5): p. e63757.

14. Wang, D., H. Umekawa, and M.O. Olson, *Expression and subcellular locations of two forms of nucleolar protein B23 in rat tissues and cells*. Cell Mol Biol Res, 1993. **39**(1): p. 33-42.
15. Borer, R.A., et al., *Major nucleolar proteins shuttle between nucleus and cytoplasm*. Cell, 1989. **56**(3): p. 379-90.
16. Okuwaki, M., *The structure and functions of NPM1/Nucleophosmin/B23, a multifunctional nucleolar acidic protein*. J Biochem, 2008. **143**(4): p. 441-8.
17. Bischof, D., et al., *Role of the nucleophosmin (NPM) portion of the non-Hodgkin's lymphoma-associated NPM-anaplastic lymphoma kinase fusion protein in oncogenesis*. Mol Cell Biol, 1997. **17**(4): p. 2312-25.
18. Palmer, R.H., et al., *Anaplastic lymphoma kinase: signalling in development and disease*. Biochem J, 2009. **420**(3): p. 345-61.
19. Barreca, A., et al., *Anaplastic lymphoma kinase in human cancer*. J Mol Endocrinol, 2011. **47**(1): p. R11-23.
20. Chiarle, R., et al., *The anaplastic lymphoma kinase in the pathogenesis of cancer*. Nat Rev Cancer, 2008. **8**(1): p. 11-23.
21. Zamo, A., et al., *Anaplastic lymphoma kinase (ALK) activates Stat3 and protects hematopoietic cells from cell death*. Oncogene, 2002. **21**(7): p. 1038-47.
22. Zhang, Q., et al., *Multilevel dysregulation of STAT3 activation in anaplastic lymphoma kinase-positive T/null-cell lymphoma*. J Immunol, 2002. **168**(1): p. 466-74.
23. Levy, D.E. and J.E. Darnell, Jr., *Stats: transcriptional control and biological impact*. Nat Rev Mol Cell Biol, 2002. **3**(9): p. 651-62.
24. Amin, H.M., et al., *Inhibition of JAK3 induces apoptosis and decreases anaplastic lymphoma kinase activity in anaplastic large cell lymphoma*. Oncogene, 2003. **22**(35): p. 5399-407.
25. Anastasov, N., et al., *C/EBPbeta expression in ALK-positive anaplastic large cell lymphomas is required for cell proliferation and is induced by the STAT3 signaling pathway*. Haematologica, 2010. **95**(5): p. 760-7.
26. Chiarle, R., et al., *Stat3 is required for ALK-mediated lymphomagenesis and provides a possible therapeutic target*. Nat Med, 2005. **11**(6): p. 623-9.
27. Zhang, Q., et al., *STAT3- and DNA methyltransferase 1-mediated epigenetic silencing of SHP-1 tyrosine phosphatase tumor suppressor gene in malignant T lymphocytes*. Proc Natl Acad Sci U S A, 2005. **102**(19): p. 6948-53.
28. Honorat, J.F., et al., *SHP1 tyrosine phosphatase negatively regulates NPM-ALK tyrosine kinase signaling*. Blood, 2006. **107**(10): p. 4130-8.

29. Han, Y., et al., *Loss of SHP1 enhances JAK3/STAT3 signaling and decreases proteasome degradation of JAK3 and NPM-ALK in ALK+ anaplastic large-cell lymphoma*. Blood, 2006. **108**(8): p. 2796-803.
30. Han, Y., et al., *Restoration of shp1 expression by 5-AZA-2'-deoxycytidine is associated with downregulation of JAK3/STAT3 signaling in ALK-positive anaplastic large cell lymphoma*. Leukemia, 2006. **20**(9): p. 1602-9.
31. Stein, H., et al., *CD30(+) anaplastic large cell lymphoma: a review of its histopathologic, genetic, and clinical features*. Blood, 2000. **96**(12): p. 3681-95.
32. Cools, J., et al., *Identification of novel fusion partners of ALK, the anaplastic lymphoma kinase, in anaplastic large-cell lymphoma and inflammatory myofibroblastic tumor*. Genes Chromosomes Cancer, 2002. **34**(4): p. 354-62.
33. Colleoni, G.W., et al., *AT1C-ALK: A novel variant ALK gene fusion in anaplastic large cell lymphoma resulting from the recurrent cryptic chromosomal inversion, inv(2)(p23q35)*. Am J Pathol, 2000. **156**(3): p. 781-9.
34. Hernandez, L., et al., *TRK-fused gene (TFG) is a new partner of ALK in anaplastic large cell lymphoma producing two structurally different TFG-ALK translocations*. Blood, 1999. **94**(9): p. 3265-8.
35. Tort, F., et al., *Molecular characterization of a new ALK translocation involving moesin (MSN-ALK) in anaplastic large cell lymphoma*. Lab Invest, 2001. **81**(3): p. 419-26.
36. Lamant, L., et al., *A new fusion gene TPM3-ALK in anaplastic large cell lymphoma created by a (1;2)(q25;p23) translocation*. Blood, 1999. **93**(9): p. 3088-95.
37. Meech, S.J., et al., *Unusual childhood extramedullary hematologic malignancy with natural killer cell properties that contains tropomyosin 4--anaplastic lymphoma kinase gene fusion*. Blood, 2001. **98**(4): p. 1209-16.
38. Lamant, L., et al., *Non-muscle myosin heavy chain (MYH9): a new partner fused to ALK in anaplastic large cell lymphoma*. Genes Chromosomes Cancer, 2003. **37**(4): p. 427-32.
39. Touriol, C., et al., *Further demonstration of the diversity of chromosomal changes involving 2p23 in ALK-positive lymphoma: 2 cases expressing ALK kinase fused to CLTCL (clathrin chain polypeptide-like)*. Blood, 2000. **95**(10): p. 3204-7.
40. Hallberg, B. and R.H. Palmer, *Mechanistic insight into ALK receptor tyrosine kinase in human cancer biology*. Nat Rev Cancer, 2013. **13**(10): p. 685-700.
41. Ferreri, A.J., et al., *Anaplastic large cell lymphoma, ALK-positive*. Crit Rev Oncol Hematol, 2012. **83**(2): p. 293-302.
42. Ferreri, A.J., et al., *Anaplastic large cell lymphoma, ALK-negative*. Crit Rev Oncol Hematol, 2013. **85**(2): p. 206-15.

43. Pulford, K., et al., *The emerging normal and disease-related roles of anaplastic lymphoma kinase*. Cell Mol Life Sci, 2004. **61**(23): p. 2939-53.
44. Falini, B., *Anaplastic large cell lymphoma: pathological, molecular and clinical features*. Br J Haematol, 2001. **114**(4): p. 741-60.
45. Tian, Z.G., et al., *In vivo antitumor effects of unconjugated CD30 monoclonal antibodies on human anaplastic large-cell lymphoma xenografts*. Cancer Res, 1995. **55**(22): p. 5335-41.
46. Turturro, F., et al., *Adenovirus-p53-mediated gene therapy of anaplastic large cell lymphoma with t(2;5) in a nude mouse model*. Gene Ther, 2000. **7**(11): p. 930-3.
47. Christensen, J.G., et al., *Cytoreductive antitumor activity of PF-2341066, a novel inhibitor of anaplastic lymphoma kinase and c-Met, in experimental models of anaplastic large-cell lymphoma*. Mol Cancer Ther, 2007. **6**(12 Pt 1): p. 3314-22.
48. Kwak, E.L., et al., *Anaplastic lymphoma kinase inhibition in non-small-cell lung cancer*. N Engl J Med, 2010. **363**(18): p. 1693-703.
49. Ou, S.H., et al., *Rapid and dramatic radiographic and clinical response to an ALK inhibitor (crizotinib, PF02341066) in an ALK translocation-positive patient with non-small cell lung cancer*. J Thorac Oncol, 2010. **5**(12): p. 2044-6.
50. Laimer, D., et al., *PDGFR blockade is a rational and effective therapy for NPM-ALK-driven lymphomas*. Nat Med, 2012. **18**(11): p. 1699-704.
51. van Holde, K.E., *Chromatin*. 1988, Berlin: Springer.
52. Davey, C.A., et al., *Solvent mediated interactions in the structure of the nucleosome core particle at 1.9 a resolution*. J Mol Biol, 2002. **319**(5): p. 1097-113.
53. Cheung, P., C.D. Allis, and P. Sassone-Corsi, *Signaling to chromatin through histone modifications*. Cell, 2000. **103**(2): p. 263-71.
54. Wolffe, A.P., *Chromatin structure and function*. Vol. 2. 1995, San Diego: Academic Press.
55. Cheung, W.L., et al., *Apoptotic phosphorylation of histone H2B is mediated by mammalian sterile twenty kinase*. Cell, 2003. **113**(4): p. 507-17.
56. Krishnamoorthy, T., et al., *Phosphorylation of histone H4 Ser1 regulates sporulation in yeast and is conserved in fly and mouse spermatogenesis*. Genes Dev, 2006. **20**(18): p. 2580-92.
57. Metzger, E., et al., *Phosphorylation of histone H3 at threonine 11 establishes a novel chromatin mark for transcriptional regulation*. Nat Cell Biol, 2008. **10**(1): p. 53-60.

58. Shimada, M., et al., *Chk1 is a histone H3 threonine 11 kinase that regulates DNA damage-induced transcriptional repression*. Cell, 2008. **132**(2): p. 221-32.
59. Eckhart, W., M.A. Hutchinson, and T. Hunter, *An activity phosphorylating tyrosine in polyoma T antigen immunoprecipitates*. Cell, 1979. **18**(4): p. 925-33.
60. Hunter, T., *Tyrosine phosphorylation: thirty years and counting*. Curr Opin Cell Biol, 2009. **21**(2): p. 140-6.
61. Krishnan, N., et al., *Dephosphorylation of the C-terminal tyrosyl residue of the DNA damage-related histone H2A.X is mediated by the protein phosphatase eyes absent*. J Biol Chem, 2009. **284**(24): p. 16066-70.
62. Xiao, A., et al., *WSTF regulates the H2A.X DNA damage response via a novel tyrosine kinase activity*. Nature, 2009. **457**(7225): p. 57-62.
63. Cook, P.J., et al., *Tyrosine dephosphorylation of H2AX modulates apoptosis and survival decisions*. Nature, 2009. **458**(7238): p. 591-6.
64. Singh, R.K., et al., *Histone levels are regulated by phosphorylation and ubiquitylation-dependent proteolysis*. Nat Cell Biol, 2009. **11**(8): p. 925-33.
65. Dawson, M.A., et al., *JAK2 phosphorylates histone H3Y41 and excludes HP1alpha from chromatin*. Nature, 2009. **461**(7265): p. 819-22.
66. Mahajan, K., et al., *H2B Tyr37 phosphorylation suppresses expression of replication-dependent core histone genes*. Nat Struct Mol Biol, 2012. **19**(9): p. 930-7.
67. Singh, R.K. and A. Gunjan, *Histone tyrosine phosphorylation comes of age*. Epigenetics, 2011. **6**(2): p. 153-160.
68. Burley, S.K. and G.A. Petsko, *Aromatic-aromatic interaction: a mechanism of protein structure stabilization*. Science, 1985. **229**(4708): p. 23-8.
69. Ausio, J., *Histone variants--the structure behind the function*. Brief Funct Genomic Proteomic, 2006. **5**(3): p. 228-43.
70. Rogakou, E.P., et al., *DNA double-stranded breaks induce histone H2AX phosphorylation on serine 139*. J Biol Chem, 1998. **273**(10): p. 5858-68.
71. Burma, S., et al., *ATM phosphorylates histone H2AX in response to DNA double-strand breaks*. J Biol Chem, 2001. **276**(45): p. 42462-7.
72. Stewart, G.S., et al., *MDC1 is a mediator of the mammalian DNA damage checkpoint*. Nature, 2003. **421**(6926): p. 961-6.
73. Goldberg, M., et al., *MDC1 is required for the intra-S-phase DNA damage checkpoint*. Nature, 2003. **421**(6926): p. 952-6.

74. Stucki, M., *Histone H2A.X Tyr142 phosphorylation: a novel sWItCH for apoptosis?* DNA Repair (Amst), 2009. **8**(7): p. 873-6.
75. Dawson, M.A., et al., *Three distinct patterns of histone H3Y41 phosphorylation mark active genes.* Cell Rep, 2012. **2**(3): p. 470-7.
76. Aoyagi, S., et al., *Nucleosome remodeling by the human SWI/SNF complex requires transient global disruption of histone-DNA interactions.* Mol Cell Biol, 2002. **22**(11): p. 3653-62.
77. Lee, C.K., et al., *Evidence for nucleosome depletion at active regulatory regions genome-wide.* Nat Genet, 2004. **36**(8): p. 900-5.
78. Amanchy, R., et al., *A curated compendium of phosphorylation motifs.* Nat Biotechnol, 2007. **25**(3): p. 285-6.
79. Hornbeck, P.V., et al., *PhosphoSitePlus: a comprehensive resource for investigating the structure and function of experimentally determined post-translational modifications in man and mouse.* Nucleic Acids Res, 2012. **40**(Database issue): p. D261-70.
80. Mason, D.Y., et al., *Nucleolar localization of the nucleophosmin-anaplastic lymphoma kinase is not required for malignant transformation.* Cancer Res, 1998. **58**(5): p. 1057-62.
81. Liu, Q.R. and P.K. Chan, *Formation of nucleophosmin/B23 oligomers requires both the amino- and the carboxyl-terminal domains of the protein.* Eur J Biochem, 1991. **200**(3): p. 715-21.
82. Lamant, L., et al., *High incidence of the t(2;5)(p23;q35) translocation in anaplastic large cell lymphoma and its lack of detection in Hodgkin's disease. Comparison of cytogenetic analysis, reverse transcriptase-polymerase chain reaction, and P-80 immunostaining.* Blood, 1996. **87**(1): p. 284-91.
83. Wetzler, M., et al., *Subcellular localization of Bcr, Abl, and Bcr-Abl proteins in normal and leukemic cells and correlation of expression with myeloid differentiation.* J Clin Invest, 1993. **92**(4): p. 1925-39.
84. Fischle, W., et al., *Regulation of HP1-chromatin binding by histone H3 methylation and phosphorylation.* Nature, 2005. **438**(7071): p. 1116-22.
85. Ewen, M.E., *Where the cell cycle and histones meet.* Genes Dev, 2000. **14**(18): p. 2265-70.
86. Schwartz, D. and S.P. Gygi, *An iterative statistical approach to the identification of protein phosphorylation motifs from large-scale data sets.* Nat Biotechnol, 2005. **23**(11): p. 1391-8.
87. Rush, J., et al., *Immunoaffinity profiling of tyrosine phosphorylation in cancer cells.* Nat Biotechnol, 2005. **23**(1): p. 94-101.

8 APPENDIX

8.1 Acknowledgements

First, I want to thank my supervisor Dr. Gerda Egger, who gave me the opportunity to conduct my master thesis in her lab. Thank you for providing practical and theoretical support, as well as encouragement, throughout the course of my project.

I want to express my deepest gratitude to my colleagues Melanie and Elisa from the Egger lab for their scientific input and assistance. I also want to thank all other members of the Clinical Pathology department for their help and for making my stay at the AKH a unique and memorable experience. Thank you all for the great conversation during coffee breaks or Friday evening lab meetings and for cheering me up after failed experiments.

Personally, I would like to thank my boyfriend Bernhard for being there when I needed someone to talk to. I know how hard it is to listen to all the science and lab stuff, so thank you for your patience!

I also want to thank my friends for their support and for making my time as a student so great and unforgettable. Special thanks go to Philipp for initially awakening my enthusiasm for genetics and for providing moral and scientific support, no matter how busy he was with his own work.

Finally I want to thank my family: my brother Philip and, of course, my parents, who have encouraged me throughout the course of my studies. Without their support I would not have been able to complete this work.

8.2 Curriculum Vitae

Julia Hacker

EDUCATION

Master's program "Genetics and Developmental Biology"

University of Vienna, Austria
since 2011

Erasmus exchange program

Uppsala University, Sweden
09/2012 – 01/2013

Bachelor's program "Biology"

University of Vienna
2007 – 2010

High school Tulln an der Donau

1999 – 2007

Primary school Absdorf

1995 – 1999

RESEARCH EXPERIENCE

Master's project

Medical University of Vienna: Group of Gerda Egger
Project: Identification of histones as phospho-tyrosine targets of the ALK kinase in anaplastic large cell lymphoma
02/2013 – 10/2013

Research project

Uppsala University: Group of Jan Dumanski
Project: Somatic variation in breast cancer
09/2012 – 01/2013

Research project

Stowers Institute for Medical Research, Kansas City: Group of Matthew Gibson
Project: Establishment of an inducible gene expression system in the sea anemone *Nematostella vectensis*
05/2012 – 07/2012

Research project

University of Vienna: Group of Günther Pass

Project: Intraspecific variation in the *Rps5* gene in myriapods

11/2010 – 01/2011

Bachelor's project

University of Vienna: Department of Population Ecology

Project: DNA Barcoding in papilinoidean caterpillars

11/2009

SCHOLARSHIPS

Performance Fellowship of the University of Vienna 2009 and 2010

Erasmus Scholarship 2012